7

Alfvén Waves Related to Moon–Magnetosphere Interactions

Bertrand Bonfond[1] and Ali Sulaiman[2]

ABSTRACT

The electro–dynamic interactions between moons and the magnetosphere of their host planets have been investigated since the mid-20th century, and the implication of the Alfvén waves was recognized right away. However, in the first models, Alfvén waves were only considered as current carriers. It is only after the Voyager missions that the possibility of complex reflection patterns was considered and their ability to accelerate particles became fully appreciated only recently. In this chapter, we review the history of our understanding of the various cases of moon–magnetosphere interactions in our Solar System. The presence of the largest of these moons in the stream of the magnetospheric plasma generates powerful large-scale Alfvén waves, which can break up into smaller scales, reflect off density gradients and accelerate particles, which ultimately impact the atmosphere of the planet to generate auroras and trigger radio emissions. The best known case is the Io–Jupiter interaction, since its observational signatures are the richest and most obvious. As our means of investigation have improved, signatures of similar interactions have also been discovered for the other Galilean moons, as well as for moons orbiting Saturn. Interestingly, similar interactions can occur on rare occasions between the planets themselves and the solar wind, and most likely take place in exo-planetary systems as well.

7.1. HISTORY OF THE MOON–MAGNETOSPHERE INTERACTIONS

This chapter deals with a particular type of phenomenon involving Alfvén waves throughout the Solar System, the moon–magnetosphere interactions. As we will discuss further, the motion of a moon through the magnetospheric plasma can excite powerful Alfvén waves propagating in both directions along the magnetic field lines toward the host planet and generate spectacular auroral phenomena. Furthermore, the peculiar geometries of these systems sometimes allow clear disentanglement of the different steps of the process, from the local Alfvén wave generation at the moons, to their intense signature in the radio emissions, passing through their filamentation via a turbulent cascade, their reflection at density gradients, and their interaction with charged particles, making them fascinating plasma physics laboratories.

In most cases in our Solar System, the regime of the moon–magnetosphere interaction is sub-Alfvénic, i.e., the relative velocity between the incoming plasma and the obstacle v_0 is lower than the local Alfvén speed

$$v_A = \frac{B}{\sqrt{\mu_0 \rho}},$$

where B is the magnetic field strength, μ_0 is vacuum permeability, and ρ is the plasma mass density; in other words, the Alfvén Mach number

$$M_A = \frac{v_0 \sqrt{\mu_0 \rho}}{B},$$

[1] *STAR Institute, University of Liège, Liège, Belgium*
[2] *School of Physics and Astronomy, University of Minnesota, Minneapolis, MN, USA*

Alfvén Waves Across Heliophysics: Progress, Challenges, and Opportunities, Geophysical Monograph 285, First Edition.
Edited by Andreas Keiling.

DOI: 10.1002/9781394195985.ch07

where v_0 is the relative velocity between the moon and the magnetospheric plasma, is lower than one (with the exception of Titan, our Moon, and Callisto). The nature of the interaction would not change abruptly beyond this threshold, but the amplitude of the far-field magnetic disturbance decreases rapidly as the Alfvén Mach number increases (Ridley, 2007; Sarantos & Slavin, 2009). An illustration of this transition can be found in Figure 7.1, which shows results from a magneto-hydrodynamic simulation of the interaction between a magnetized planet and the solar wind for different Alfvén Mach numbers between 8.2 and 0.7. It can be seen that the magnetosphere transforms into Alfvén wings, carrying more and more energy along the Z-axis (i.e., along the magnetic field lines). Saur (2021) provided a thorough review of the moon–magnetosphere interaction, with an emphasis on the theory of the local interaction. Hence, the present review is rather focused on the observations and the way they advanced our understanding of the processes involved.

It is important to distinguish between two types of obstacles generating Alfvén waves: the mechanical obstacles and the electromagnetic obstacles. The former can be further separated into 1) inert obstacles, for which the moon's surface absorbs particles from the incoming plasma and generating a low density wake downstream, and 2) mass-loading obstacles, for which moons with a significant atmosphere modify the momentum of the incoming plasma as the newly ionized particles drag the field lines before being accelerated. On the other hand, electromagnetic obstacles can be formed by either an intrinsic or an induced magnetic field, which can itself originate either in the ionosphere, in a sub-surface ocean, or in an asthenosphere (a ductile and partially melted layer below a rocky crust) and in a metallic core. In practice, the effects are combined, as a moon can both have an atmosphere and a sub-surface conductive layer (e.g., Europa; see Section 7.2.1).

The case of Io and Jupiter is probably the most prominent example, at least historically speaking. The first hint of the peculiar relationship between Io and Jupiter came from Bigg (1964), who noted that the decametric radio emissions from Jupiter were modulated by Io's position both along its orbit and in the Jovian magnetic field. At the same time, but much closer to the Earth, the first experimental telecommunication satellite, a 30-m wide balloon named Echo 1, was losing altitude at a larger rate than expected. Drell et al. (1965) suggested an original theory to explain this strange behavior: since Echo 1 basically consisted of a giant sphere of electrically conductive metal, it was electro-magnetically interacting with the terrestrial magnetic field. As the flux tubes filled with magnetospheric plasma move relative to the spacecraft, an electric field forms across it perpendicular to both the motion direction and the magnetic field. Since the body of the spacecraft is conductive, an electric current would flow across the spacecraft. The Lorenz force, perpendicular to both the magnetic field and the current direction would be oriented in the direction opposite to Echo 1's velocity vector, would then slow the spacecraft down. At the same time, the magnetic field associated with this transverse electric current would shield the object from the external magnetic field. The interaction between the spacecraft and the surrounding plasma generates Alfvén waves, which propagate along the magnetic field lines (forming a structure called Alfvén wings) and which carry field-aligned currents, thus allowing for the current flowing across the spacecraft to close outside of it.

While the unexpected slowing down of Echo 1 turned out to be more easily explained by an underestimation of the radiation pressure and atmospheric drag at its orbiting altitude, the idea of an electric current associated with the motion of a conductive celestial body disturbing the ambient plasma flow proved to be relevant and attracted other researchers, who proposed that a similar system could be at play at Io. A first scenario was drafted by Piddington and Drake (1968), followed by a more detailed discussion by Goldreich and Lynden-Bell (1969). This first model is called the "unipolar inductor" model. It should be noted that, while this model was opposed to the "Alfvén wings" model later on, it was already clear in the authors' minds that the current was carried along the magnetic field lines via Alfvén waves. Furthermore, the concept of Alfvén wings was already defined by Drell et al. (1965). However, in the unipolar inductor model, as the Alfvén velocity was expected to be close to the speed of light because the magnetosphere plasma was expected to be extremely tenuous, the Alfvén waves reflecting on the Jovian ionosphere would directly fall back on Io before the satellite could move significantly along its orbit. Because feedback would get established very rapidly, the interaction could then be modeled as a direct current loop. The motion of Io, considered as an infinitely conductive body, across Jupiter's North-South aligned magnetic field lines, induces a motional electric field oriented radially in the anti-Jovian direction, and the current flows in the same direction. It would then connect to the Jovian ionosphere along the magnetic field lines (see Figure 7.2). Initial speculations suggested that the current would flow inside Io's interior, but later iterations (Webster et al., 1972) considered that the current would rather flow as Pedersen and Hall currents in Io's ionosphere. Indeed, the existence of such an ionosphere was later demonstrated through Pioneer 10 radio occultations (Kliore et al., 1975). One of the important characteristics of this family of models is that the current intensity is essentially limited by the Pedersen conductivity in Jupiter's ionosphere.

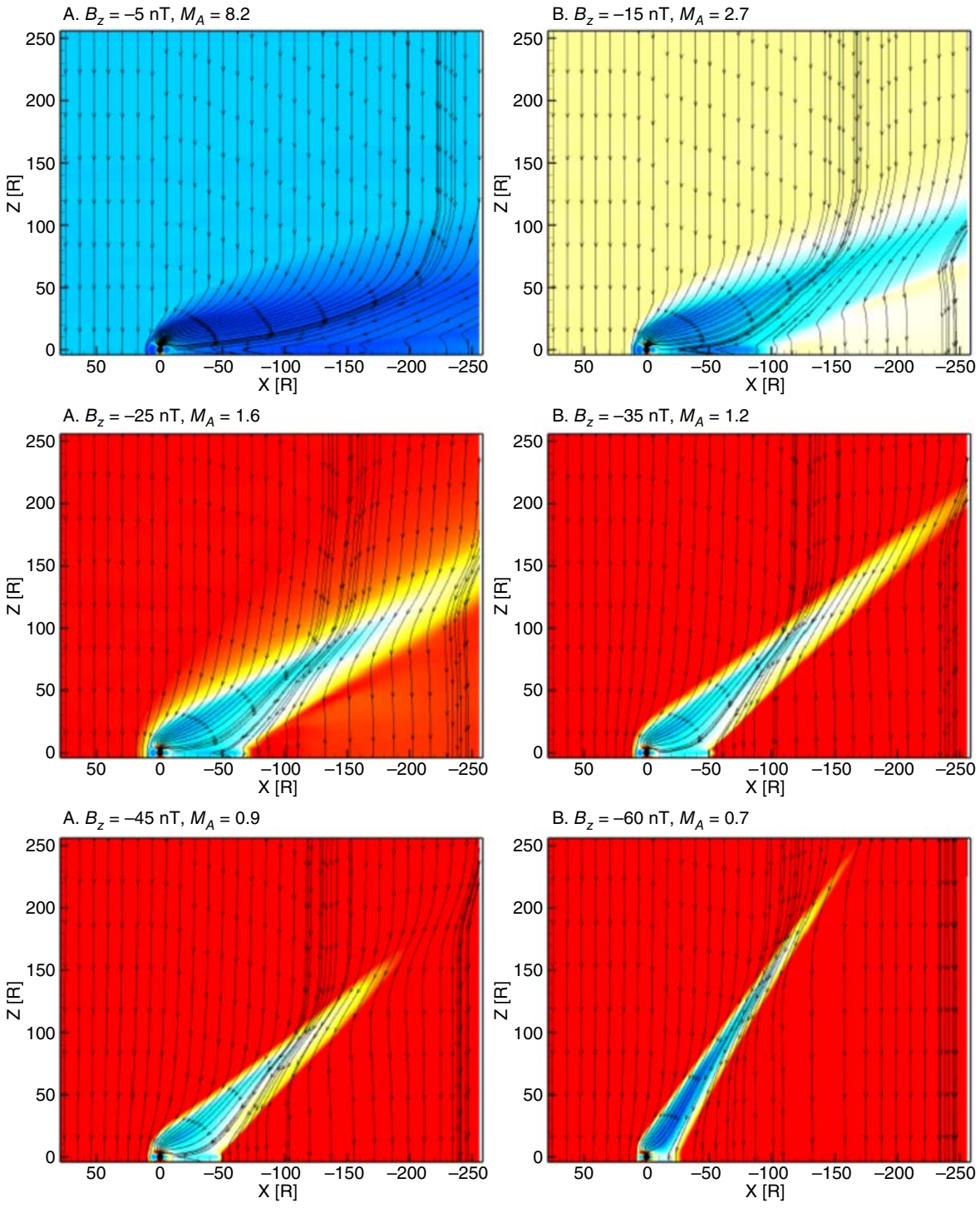

Figure 7.1 Outputs from magneto-hydrodynamic simulations of the interaction between the solar wind and the Earth. The colors represent the electric field (dark blue is 0 mV/m and red is 10 mV/m) and the lines represent the magnetic field. Images of the velocity fields would display similar features. Starting from typical conditions and an Alfvén Mach number (M_A) of 8.2, we can see that the magnetotail transforms progressively into Alfvén wings as the M_A decreases. When Alfvén wings form, energy, and currents can be efficiently carried away from the interaction site over long distances. Source: Reproduced Ridley (2007) / European Geosciences Union / CC BY 4.0.

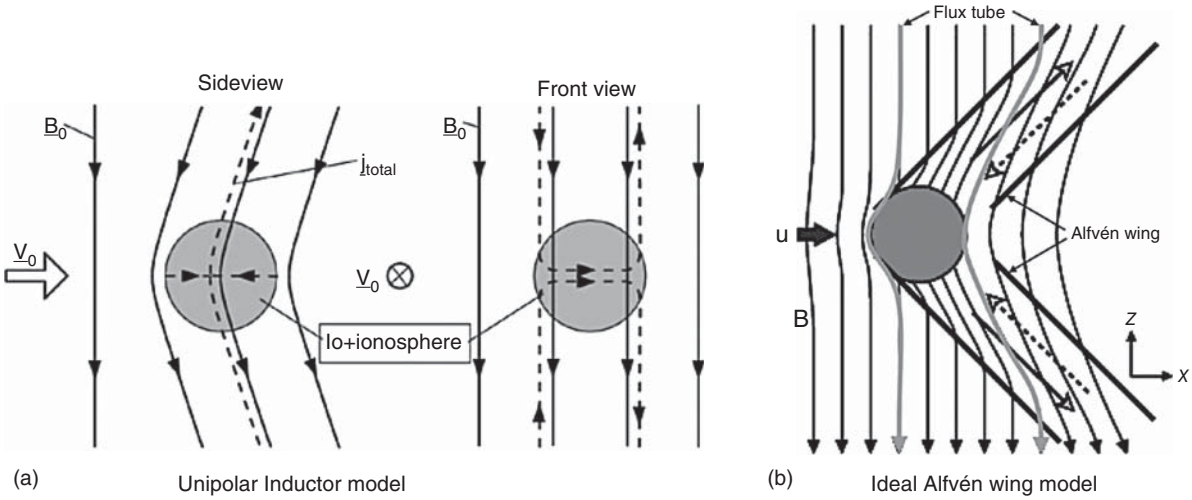

Figure 7.2 (a) Schematic of the local interaction in the case of immediate feedback from the planet's ionosphere to the moon (the "unipolar inductor"). (b) Schematic of the local interaction in the case where there is no feedback from the planet's ionosphere to the moon (the "ideal Alfvén wing model"). In the first case, the Io flux tube and the Alfvén wing are identical, while in the second, they are decoupled. Source: Adapted from Saur (2004) and Kivelson et al. (2004).

When Voyager 1 performed a close encounter with Io on 5 March 1972 (closest distance: 20500 km), its trajectory was originally designed to cross the southern Io Alfvén wing, but it only skimmed it from the upstream side (Ness et al., 1979). The magnetometer, however, measured a disturbance of the magnetic field consistent with 5 MA current, a number of the same order of magnitude as the initial estimates of ∼ 1 MA by Goldreich and Lynden-Bell (1969). Furthermore, the Voyager probes revealed evidence of Io's intense volcanism and the presence of a dense plasma torus along Io's orbit. Since the Alfvén velocity is inversely proportional to the square root of the mass density, the validity of the direct current hypothesis came under question, because the Alfvén travel time could become longer than the time taken by Io to move by its diameter in the plasma's reference frame. Neubauer (1980) expanded the linear model of Drell et al. (1965) into a fully non-linear model. He noted that, in this situation, the current would flow along the Alfvén characteristics, which are tilted, not only relative to the unperturbed field lines but to the perturbed field lines as well (contrary to the expectations of the DC current model, see Figure 7.2). Moreover, the non-linear Alfvén current tubes (the Alfvén wings) have a non-negligible resistance and, in this theoretical frame, since there is no feedback from Jupiter's ionosphere, it is this Alfvénic resistance that controls the amount of current, rather than the Pedersen conductance in Jupiter's ionosphere. With the Alfvén wings being distinct from the Io flux tube, the Alfvén waves' reflections on the density gradient outside of the plasma torus, or in Jupiter's ionosphere, would end up forming a complex pattern, possibly explaining the shape of the radio decametric wave spectrograms (Bagenal, 1983; Gurnett & Goertz, 1981). At the same time, since Io's atmosphere is the source of the plasma torus, another phenomenon in addition to the unipolar inductor/mass loading mechanism was proposed as a current generator: the pick-up current related to the newly ionized particles (Cheng & Paranicas, 1998; Goertz, 1980). As neutral atoms and molecules get ionized around Io, the electrons and ions start gyrating around the magnetic field lines in opposite directions with electrons going toward Jupiter and ions away from it. Vasyliūnas (2016), however, argued that the pick-up currents are only transient as they are almost instantaneously (i.e., on the electron-gyroperiod timescale) compensated by polarization currents. The main effect generating Alfvén waves and its associated currents is due to momentum exchange related to mass loading, since the newly ionized plasma is initially at rest relative to the moon, it exchanges momentum with the incoming plasma and slows down the resulting flow. This velocity gradient in the plasma flow results in a curl of the magnetic field and thus currents. The currents are transmitted along the field lines by Alfvén waves.

Another important discovery took place between the Voyagers flybys and the arrival of Galileo's finding of the Io auroral footprint, a set of spots magnetically connected to Io, which are followed by an extended tail along a contour mapping to Io's orbit (Figure 7.3a). Its first detection in the infrared domain (Connerney et al., 1993) was followed by its observation in the ultraviolet domain with the Hubble Space Telescope (Clarke et al., 1996; Prangé et al., 1996). On one hand, the existence

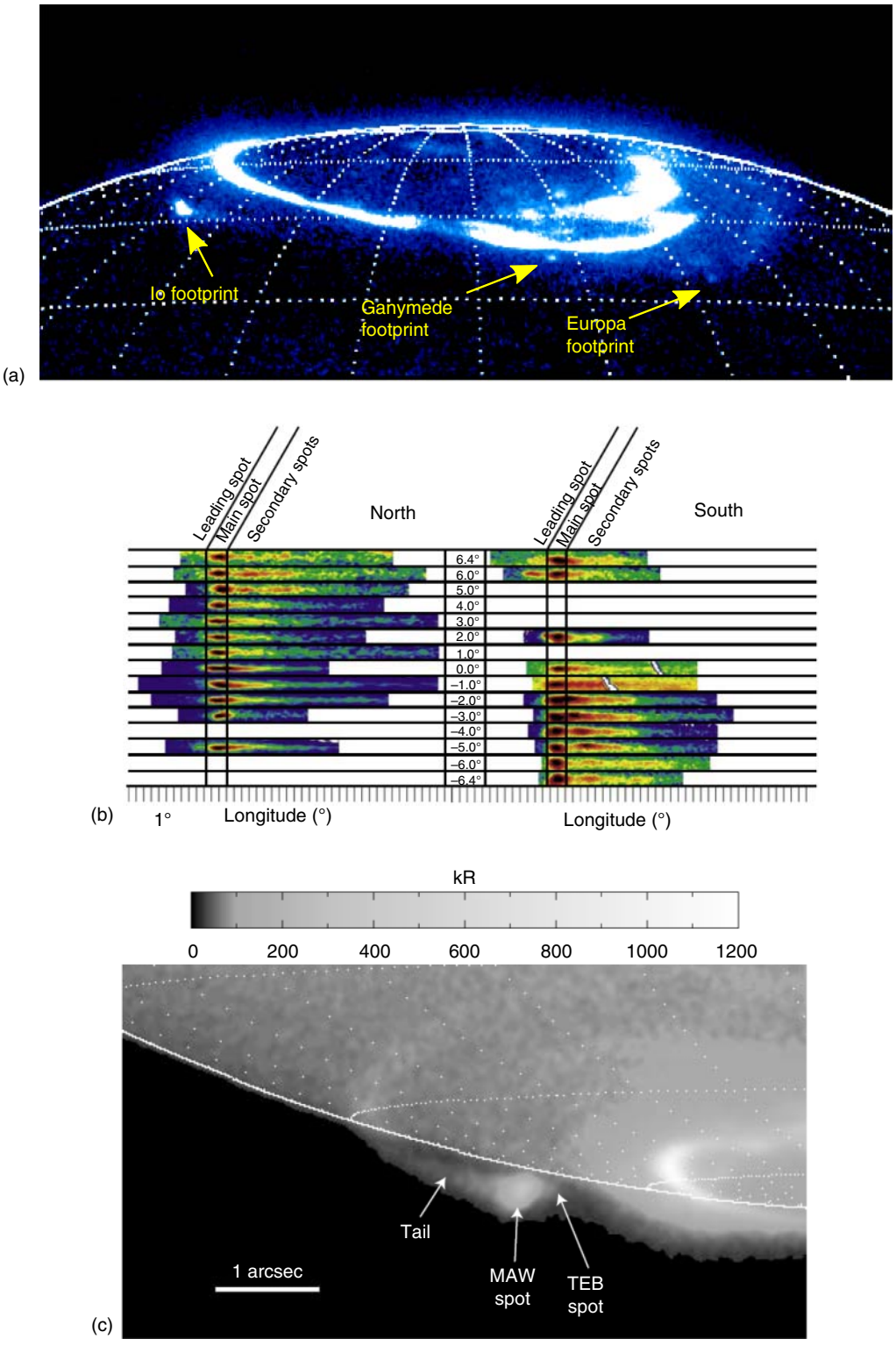

Figure 7.3 (a) Image of the northern FUV aurora of Jupiter acquired with the Hubble Space Telescope's ACS camera on 7 February 2006. The Io, Europa, and Ganymede footprints are simultaneously visible. Source: Adapted from Bonfond., 2012 / American Geophysical Union. All Rights Reserved. (b) Scheme of the Io morphology as a function of the centrifugal latitude of Io in the torus. The longitudes are not measured on the planet, but mapped to the equatorial plane along the magnetic field lines according to the VIP4 magnetic field model for an easier comparison of both hemispheres. Source: Bonfond et al. (2008) / with permission of John Wiley & Sons. (c) Example of Io footprint tail and spots observed above the limb. Source: Adapted from Bonfond., 2010 / John Wiley Sons.

of several spots (Clarke et al., 2002; Gérard et al., 2006) clearly favored a de-coupling between Io and Jupiter's ionosphere, as the multiple spots were a prediction from the Alfvén wings reflection pattern (Gurnett & Goertz, 1981; Neubauer, 1980). On the other hand, the presence of a long, continuous tail left the door open for the establishment of a steady-state direct current loop associated with acceleration of the picked-up plasma toward corotation (Hill & Vasyliūnas, 2002; Delamere et al., 2003).

Galileo's exploration of the Jovian system from December 1995 to September 2003 marked another giant leap in our understanding of the moon–magnetosphere interactions. The spacecraft performed 7 flybys of Io, 9 of Europa, 6 of Ganymede, and 9 of Callisto, sending back a wealth of particle, magnetic field, and wave data documenting the interactions. For example, at Io, Galileo revealed a wake of stagnant plasma (Frank et al., 1996) and intense bi-directional electron beams (Frank et al., 1996; Frank & Paterson, 1999; Williams & Thorne, 2003; Williams et al., 1996). This extended wake of freshly ionized plasma remains quite stagnant relative to Io (Hinson et al., 1998). Hence, this discovery led to the suggestion that the field lines disturbed by Io may still be connected to it when the Alfvén waves bounce back, hence reviving the idea of a DC current loop. Several hybrid models have then been proposed to reconcile both approaches (e.g., Crary & Bagenal, 1997; Pontius, 2002); and Neubauer (1998) as well as Saur (2004) argued that both theories were extreme cases of a more general mixed Alfvén wings theory. At Europa, Galileo identified the induced magnetic field stemming from Europa's sub-surface ocean (Kivelson et al., 2000). At Ganymede, Galileo identified the presence of a mini-magnetosphere embedded within Jupiter's one, owing to Ganymede's intrinsic magnetic field (Kivelson et al., 1998). At Callisto, Galileo also found the signature of an induced magnetic field, even if its origin, a sub-surface conductive layer, or the ionosphere, remains unclear (Hartkorn & Saur, 2017; Khurana et al., 1998). Almost a decade later, Cassini would provide a similar wealth of information regarding the Kronian moons, with the most notable example being the discovery of the neutral clouds originating from geysers on the southern pole of Enceladus (Dougherty et al., 2006; Porco et al., 2006).

Before the discovery of footprint emissions, most theoretical efforts concentrated on the generation of the Alfvén waves and on their propagation (Wright, 1987; Wright & Southwood, 1987), but little consideration was given to their dissipation and their ability to interact with particles. Indeed, in ideal magneto-hydrodynamics (MHD), Alfvén waves do not develop a parallel electric field and are thus unable to accelerate particles along the field lines (Lysak, 2023). In the framework reducing the interaction to a direct current loop, should it concern the spots or the tail, the acceleration of the auroral electrons is attributed to quasi-static potential drops located above the Jovian ionosphere, described by the Knight relationship or a variation of it adapted to Jupiter (Ergun et al., 2009; Hill and Vasyliūnas, 2002; Matsuda et al., 2012). On the other hand, models focusing on the Alfvén waves, propagation started to account for the dispersive effects of the Alfvén waves (i.e., the kinetic and inertial regimes), for which an alternating parallel electric field could develop and accelerate the charged particles in a parallel direction. Crary (1997) proposed a model in which inertial Alfvén waves would accelerate electrons along the field lines within the torus via repeated Fermi acceleration. A decade later, Jones and Su (2008) considered both kinetic and inertial effects and concluded that inertial effects would be much more efficient at accelerating the electrons in both directions along the field lines outside the torus rather than inside it. Hess et al. (2010) further refined this scenario and assessed the energy balance for each step leading to auroral emissions: the power generation, the turbulent filamentation of the waves, the power transmission through the torus boundaries, the efficiency of the electron acceleration, and their ability to finally precipitate into the atmosphere, and Hess et al. (2011) extended this analysis to Europa and Enceladus. Their model showed that the electron acceleration by inertial Alfvén waves at high latitude forms broadband bi-directional electrons beams. The electrons accelerated toward Jupiter could precipitate into the atmosphere and generate auroral emissions. The electrons accelerated away from Jupiter then cross the equatorial plane close to Io (Jacobsen et al., 2010), which explains the Galileo measurements of bi-directional electron beams during Io flybys. Part of this electron beam would remain trapped on its field line, and part of it would precipitate into the atmosphere in the other end of the field line and also generate auroral emissions. Indeed, Bonfond et al. (2008) noted that the relative motion of the Io footprint spots and the occurrence of a leading spot upstream of the brightest one was not compatible with a scenario only relying on reflected Alfvén waves, but could be explained if electrons accelerated anti-planetward in one hemisphere could precipitate in the opposite hemisphere (see Figures 7.3b and 7.4). The brightest spot is generally associated with the main Alfvén wing (MAW), originating directly from Io. A second spot, always located downstream of the first one, is associated with the first reflection of the Alfvén wing (RAW). Its distance to the MAW spot is minimum in the northern hemisphere when Io is close to the southern edge of the torus (Hinton et al., 2019) (Figure 7.4). A third spot is associated with electrons accelerated away from Jupiter in one hemisphere and precipitating in the opposite hemisphere (Trans-hemispheric Electron Beam,

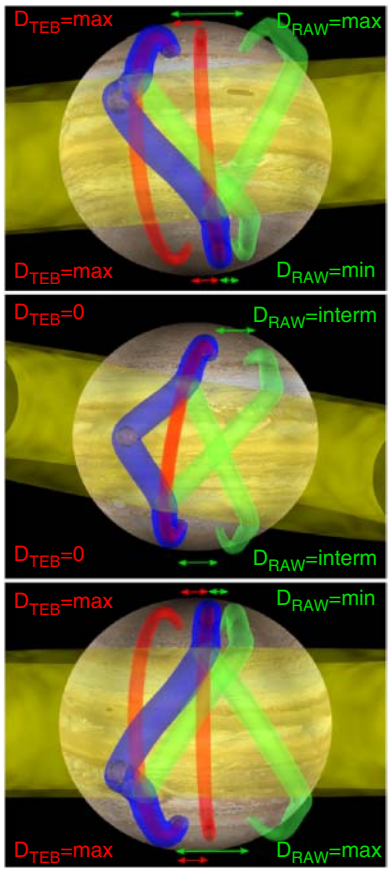

Figure 7.4 Schematic presentation of the Alfvén wing reflection pattern and Trans-hemispheric Electron Beams (TEB, shown in red) when Io is in its northern-most (top), central (middle), or southern-most position relative to the plasma torus (shown in yellow). The main Alfvén wing (MAW) is shown in blue and the reflected Alfvén wing (RAW) is shown in green. On the top panel, in the North, the distance between the MAW spot and the TEB spot (D_{TEB}) is maximal as well as the distance between the MAW spot and the RAW spot (D_{RAW}). Note that in a linear case, $max(D_{RAW}) \sim 2max(D_{TEB})$. In the South, D_{TEB} is also maximal, but the TEB spot is now upstream of the MAW spot. D_{RAW} reaches its minimum. When Io is in the center of the torus (middle panel) the situation in the two hemispheres is symmetric, and the TEB spots are merged with the MAW spots. Source: Bonfond et al., 2017b / with permission of Elsevier.

TEB spot). Because electrons travel faster than Alfvén waves, the TEB spot is located upstream of the MAW spot in the northern hemisphere when Io is close to the southern edge of the torus (see Figure 7.4) (Bonfond et al., 2008). The altitude of the brightness peak is 850–900 km (Bonfond, 2010) (Figure 7.3c) and its vertical profile suggests a broadband energy distribution with a 1 keV mean energy. This observation constitutes another clue in favor of the Alfvénic acceleration process, since the broad vertical profile of the Io footprint main spot and tail is only compatible with a broadband, kappa-like electron energy distribution, and not with a narrow distribution as expected from a quasi-static potential drop (Bonfond et al., 2009; Bonfond, 2010; Bonfond, Saur, et al., 2017). The resulting anisotropic distributions of field-aligned electrons are unstable to the generation of plasma waves, which are commonly observed on the flux tubes connected to the Io footprint. A prominent one is the whistler-mode auroral hiss, which arises from a beam-plasma instability, undergoing wave growth via Landau resonance (e.g., Sulaiman et al., 2020). The resulting band of frequencies obeys a dispersion relation such that higher frequencies propagate at a larger angle to the background magnetic field, enabling detection of the interaction well before and after the satellite footprint flux tube is crossed (Figures 7.7 and 7.8c). Radio waves are also generated as a result of the moon–magnetosphere interaction, notably the Io Decametric Radio Emission. Here, the anisotropic electron distribution drives the cyclotron maser instability from which the growth of radio waves occurs (Zarka, 1998). The generation of a free-space mode as such enables moon–magnetosphere interactions to be detected from very remote distances (Bigg, 1964).

After Galileo's close encounters providing precious data on the local interaction, Juno's arrival at Jupiter in August 2016 offered a unique opportunity to explore the physical processes at the polar end of the field lines. While its observations confirmed the scenario inferred from remote sensing of the aurora, they also unveiled unexpected results, suggesting that the story told here is not the final word on the issue, as described in Section 7.2.1.

As discussed earlier, most of the ideas related to the generation of Alfvén waves by moon–magnetosphere interactions were motivated by observations of the Io-Jupiter system. However, the subsequent exploration of other systems revealed that the lessons learned at Io could essentially apply everywhere, even on Earth (see Section 7.2.4). It is also noteworthy that the modeling efforts reducing interactions to direct current systems are fruitful first steps, providing the correct orders of magnitude. However, at some point, they proved to be oversimplifications that obscured essential properties of the Alfvén waves, which turned out to be key to explaining the increasingly detailed observations, such as the decoupling between the Alfvén wing and the satellite flux tube, or the bi-directional broadband electron acceleration (Bonfond et al., 2008, 2009; Hess et al., 2010; Neubauer, 1980). Similar limitations have also been noted for the main auroral emissions at Jupiter (Bonfond et al., 2020).

7.2. MOON–MAGNETOSPHERE AND SIMILAR INTERACTIONS THROUGHOUT THE SOLAR SYSTEM

7.2.1. The Jovian Moons

Io

Because of the favorable combination of its intrinsic strength and relative proximity to the Earth, the Io–Jupiter electro–magnetic interaction is the easiest to scientifically investigate. Its signatures in the radio, infrared, and ultraviolet domains radiate enough energy to be observed from Earth, and Io has been visited by two spacecrafts (Voyager 1 and Galileo) and is currently explored at a close distance by Juno. The magnetic in-situ field and particle observations from Voyager 1 (Acuña et al., 1981; Belcher et al., 1981) and Galileo (Kivelson et al., 1996) provided signatures of the generation of large-scale Alfvén waves at Io. Furthermore, high-frequency/small scale fluctuations of the magnetic and electric fields (see Figure 7.5) suggested that the Alfvén waves were subject to turbulent filamentation into smaller scales, which would more easily allow the Alfvén waves to escape from the torus and trigger electron acceleration processes outside of it (Chust et al., 2005; Hess et al., 2010). Moreover, Galileo particle instruments showed the presence of bi-directional electron beams in Io's wake (Frank et al., 1996; Frank & Paterson, 1999; Williams & Thorne, 2003; Williams et al., 1996) and mono-directional above Io's poles (Mauk et al., 2001), indicative of an electron acceleration process taking place close to Jupiter. After their exit from the high-density torus, the Alfvén waves related either to the main Alfvén wing spot or to the following tail have been observed by Juno at high latitude (Gershman et al., 2019; Sulaiman et al., 2020) (Figure 7.7). Furthermore, Alfvénic Poynting fluxes in the highlatitudes were found to highly correlate with electron energy fluxes and are coupled by an efficiency (10%) that is fully consistent with acceleration from Alfvén wave filamentation via a turbulent cascade process (Hess et al., 2010; Sulaiman et al., 2023). Juno also observed the bidirectional broadband electron population (Szalay et al., 2018) expected from the models of acceleration via inertial Alfvén waves (Damiano et al., 2019; Hess et al., 2010; Jones & Su, 2008). The main difference between the electron populations related to the main Alfvén wing spot or the tail is the energy flux, rather than the energy or the pitch angle distributions (Szalay et al., 2020b). What was less expected from previous theoretical studies (e.g., Hess et al., 2013a) was the finding of proton acceleration along the Alfvén wing (Clark et al., 2020; Szalay et al., 2020c). Another surprise was the occasional identification of a double peak in the particle flux down the tail (Szalay et al., 2018) and of a split tail in the infrared images (Mura et al., 2018).

The Io auroral footprint is made up of at least 3 spots and an extended tail in the downstream direction. The spots are approximately 850 km long, which corresponds to 3–4 times the projected size of Io, <200 km wide (<2 times the projected width of Io) and 1200 km tall (full width at half maximum) (Bonfond, 2010). The relative distance between the spots evolves as Io oscillates north and south of the torus centrifugal equator. The UV-emitted power of the different spots varies with the System-III longitude of Io (System-III is a longitude system fixed with the magnetic field of Jupiter). The observed brightness results from a combination of processes (Bonfond et al., 2013b; Hess et al., 2013) and the footprint may even completely vanish when it crosses an auroral injection signature (Bonfond et al., 2012; Hess, Bonfond, & Delamere, 2013). On the other hand, Hue et al. (2019) have shown that the brightness of the main spot was not affected by the collapse of Io's atmosphere during the eclipse.

Moreover, high-resolution images of the H_3^+ auroral emissions of the footprints showed that the spots were formed of sub-structures, named sub-spots, which were fixed with the planet (contrary to the larger spots features that are moving with Io) (Moirano et al., 2021; Mura et al., 2018).

In addition to the infrared and ultraviolet domains, the morphology of the Io footprint has also been observed in the visible domain (Gladstone et al., 2007; Vasavada et al., 1999).

The precipitation of electrons into the polar atmosphere leads to a loss-cone pitch angle distribution, which is susceptible to the growth of the maser-cyclotron radio emission (Louis et al., 2017; Queinnec & Zarka, 1998). In addition to the Alfvénic acceleration, which is the main source of particle energization, evidence of upward migrating intermittent potential structures have also been highlighted by Hess et al. (2009). The recurrent formation and upward migration of these structures every 2–3 minutes may explain the short-timescale fluctuations of the Io footprint brightness (Bonfond et al., 2007; Bonfond, Hess, Gérard, et al., 2013). A visual summary of the chain of processes giving rise to the auroral footprints, together with the related plasma and radio waves, can be found on Figure 7.6.

Europa

Arising mostly from the sputtering of its icy surface by magnetospheric particles, the atmosphere and ionosphere of Europa are much less dense than Io's, leading to a weaker plasma interaction and 20 times smaller mass loss ($\sim$50kg s^{-1}) (Bagenal & Dols, 2020; Saur et al., 1999).

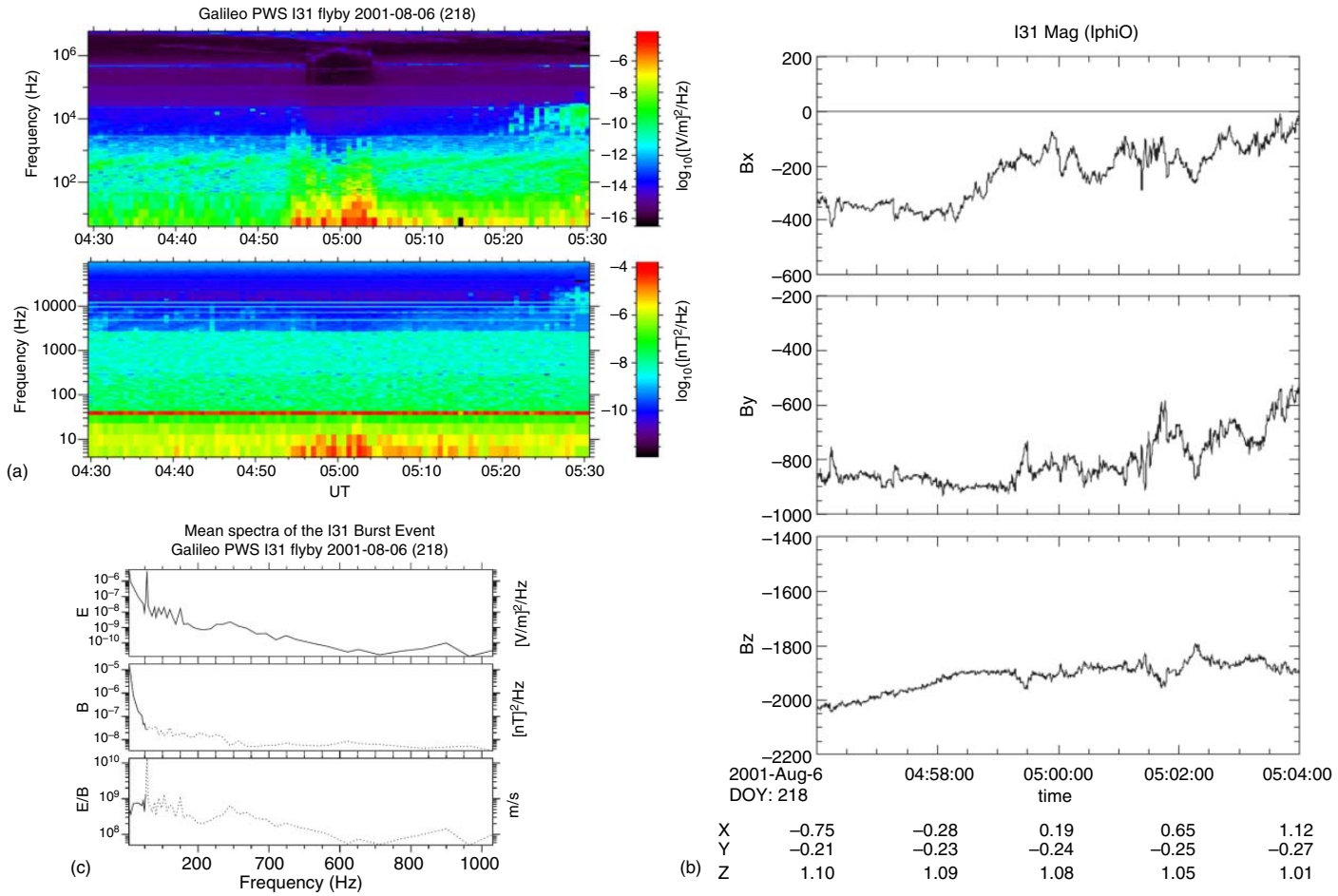

Figure 7.5 (a) Calibrated dynamic spectra of the electric field (top) and magnetic field (bottom) acquired by the PWS (Plasma Wave Subsystem) instrument on board Galileo during the I31 flyby on 7 December 1995. The Alfvén wing crossing started about 5 minutes before the closest approach (04:59:20). (b) Magnetic field observations during the crossing of the Alfvén wings during the same event, but the time interval is narrowed down to the duration of the Alfvén wing crossing. The x-axis is parallel to the unperturbed flow, the y-axis is pointing toward Jupiter and the z-axis is parallel to Jupiter's rotation axis. (c) Electric and magnetic wave spectra, and the corresponding ratio of these two quantities. In this example, it can be seen that the crossing of the Alfvén wing is accompanied with the observation of intense higher frequency waves (with most of the energy remaining below 50 Hz), which have been interpreted as the signature of turbulent filamentation of the Alfvén waves originating from Io. Source: Chust et al. (2005) / with permission of Elsevier.

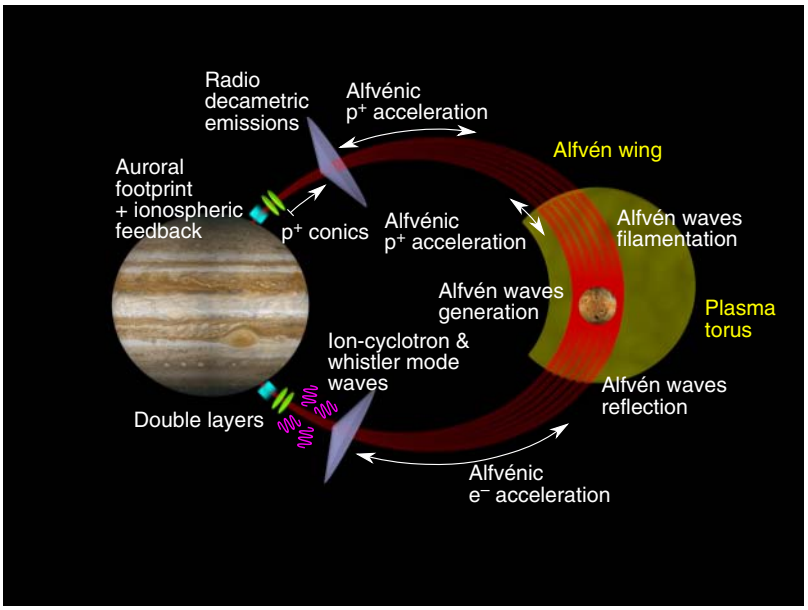

Figure 7.6 Schematic of the chain of processes arising from the Io–Jupiter electro–magnetic interaction.

However, Europa is also the source of an induced magnetic field, which is one of the most compelling evidences for the existence of its subsurface ocean (Kivelson et al., 2000). Both effects contribute to making Europa an obstacle to the stream of magnetospheric plasma and to the generation of Alfvén wings (e.g., Schilling et al., 2008). Localized sources of neutrals related to cryovolcanoes (Arnold et al., 2019; Huybrighs et al., 2020; Jia et al., 2018; Roth et al., 2014) could even cause smaller structures, called Alfvén winglets, within the larger Alfvénic structure (Blöcker et al., 2016). Moreover, evidence for an extended plasma wake, or plume, were found in the Galileo data (Eviatar & Paranicas, 2005; Kivelson et al., 1999; Kurth et al., 2001).

Juno has also crossed the magnetic field lines connected to the Europa footprint tail and intriguing differences were found compared to the observations at Io (Allegrini et al., 2020). In addition to a broadband energy distribution with a mean energy of 3.6 keV, a peak at an energy of ~ 2 keV was also found, suggesting that the electron acceleration was at least partly electrostatic. At the Jovian end of the Alfvén wings, UV auroral spots (Bonfond, Grodent, et al., 2017; Clarke et al., 2002) and a downstream tails are also occasionally observed (Bonfond, Saur, et al., 2017; Grodent et al., 2006). High-resolution images of the infrared H_3^+ emissions also showed the occasional appearance of sub-dots, similarly to Io's (Moirano et al., 2021). As shown in Figure 7.3a, the UV Europa footprint is much weaker than the Io's, and it is often hard to identify among the surrounding auroral emissions. The identification of a second spot is even rarer, and, when it could be identified, its location and motion were found consistent with those of an reflected Alfvén wing (RAW) spot (Bonfond, Grodent, et al., 2017).

While the generated power is much weaker than for Io, decametric radio emissions related to the Europa footprint have also been observed by Voyager 1 and Cassini (Louis, Lamy, Zarka, Cecconi, & Hess, 2017). The interaction between Europa and the Jovian magnetosphere will become the object of great scrutiny in the next decade with the arrival of two dedicated spacecrafts, Europa Clipper, and JUICE.

Ganymede

Ganymede is the largest moon of the Solar System (with a radius $R_G = 2634$ km) and is the only one with its own intrinsic magnetic field, which carves a magnetosphere within Jupiter's magnetosphere (Kivelson et al., 1998). It is this 2-3 R_G-wide mini-magnetosphere that forms an obstacle to the plasma flow (Neubauer, 1998; Jia et al., 2008). At the front of Ganymede's magnetosphere (i.e., the upstream side relative to the magnetospheric plasma flow), the magnetic field is anti-parallel to Jupiter's, a configuration favorable to magnetic reconnection. The transverse electric potential drop across Ganymede's magnetosphere is estimated at around 80 kV (Zhou et al., 2020), and the total current carried along the Alfvén waves lies around 0.5 MA (Lavrukhin and Alexeev, 2015). This unique configuration of a nested magnetosphere creates a variety of accelerated or trapped electron populations, either on closed field lines around Ganymede or between Ganymede and Jupiter (Frank et al., 1997; Williams, Mauk, & McEntire, 1997; Williams et al., 1997;

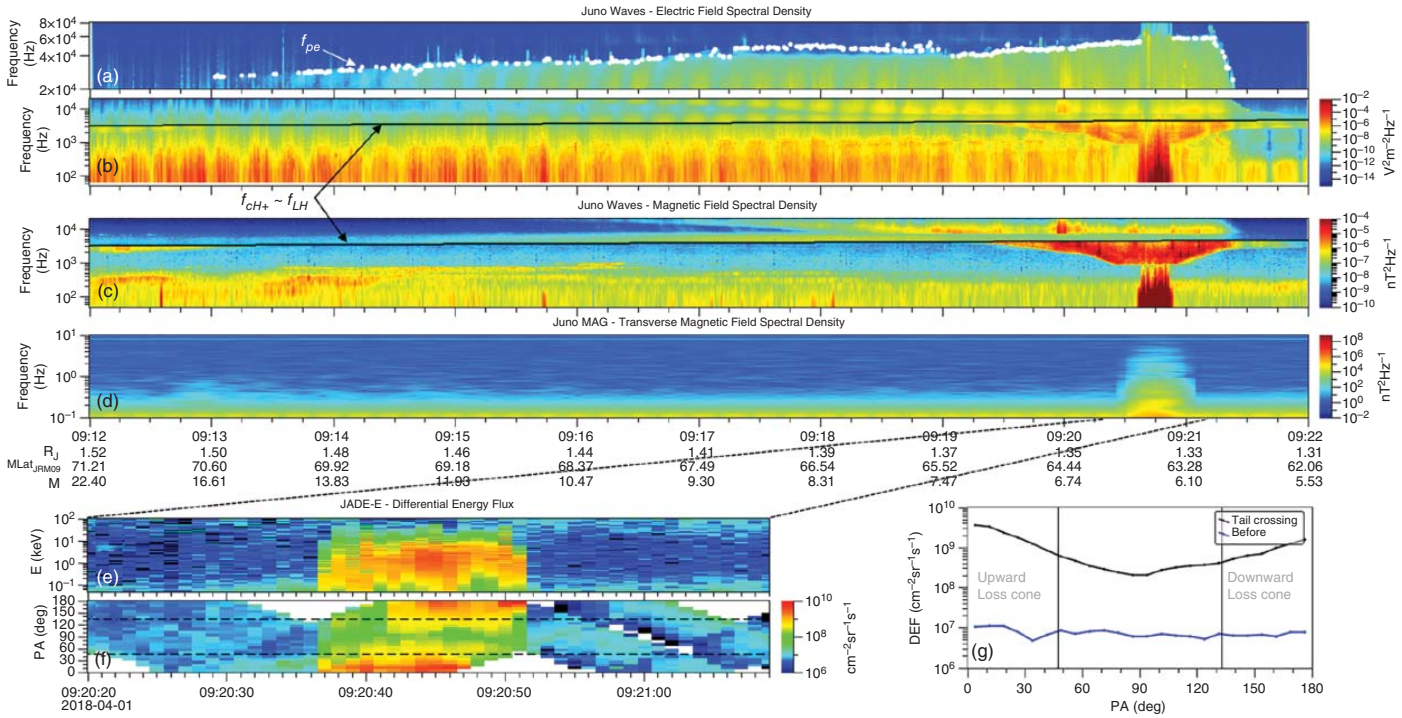

Figure 7.7 (a-d) Electric and magnetic field frequency-time spectrograms measured in the MAW revealing MHD and plasma waves across multiple scales, namely, Alfvén, ion cyclotron, and whistler modes. (e-g) Electron data revealing broadband and bidirectional distributions of electrons, likely accelerated by inertial Alfvén waves at the high latitudes, and also the source of whistler-mode waves. Source: Sulaiman et al. (2020) / with permission of John Wiley & Sons.

Williams & Mauk, 1997; Eviatar et al., 2000). Furthermore, the particles energized by magnetic reconnection at the front and tail of the magnetopause are the sources of local electrostatic and electromagnetic emissions (Gurnett et al., 1996). Galileo also measured a deceleration of the convective magnetospheric plasma flow to less than one third of rigid corotation, which is compatible with a traversal of an Alfvén wing (Eviatar et al., 1998). At high latitudes, Ganymede's auroral footprint is formed of at least two spots (Bonfond, Hess, Bagenal, et al., 2013) and an elongated tail (Bonfond, Saur, et al., 2017). The presence of such a tail while Ganymede is not subject to any significant mass loading implies that this process isn't a necessary condition for the presence of a footprint tail. It favors interpretations of the auroral footprint tails implying repeated reflections of Alfvén waves, as opposed to explanations involving the progressive acceleration of plasma in the wake. The motion of the secondary spot suggested an origin related to trans-hemispheric electron beams; an interpretation confirmed by Juno's in situ measurements when crossing field lines connected to this spot (Hue et al., 2021). On field lines connected to the TEB spot, Juno only detected weak currents in addition to the bi-directional electron beams, contrary to measurements in the tail where significant currents and strong Alfvénic activity were also found (Szalay et al., 2020a). As Juno was crossing the Ganymede footprint tail, it also encountered the source region of decametric radio emissions (Louis et al., 2020). In the high-resolution infrared images, sub-dots, similar to those observed at Io, were also reported (Mura et al., 2018). The brightness of the main spot varies according to three separate timescales: several hours, tens of minutes, and 2-3 minutes (Grodent et al., 2009). The first one is related to the passage of Ganymede through the denser core of the plasma sheet, the second probably corresponds to interactions with local plasma inhomogeneities, such as plasma injections (see also Bonfond, Grodent, et al., 2017) and the shortest one could correspond either to the time between subsequent reconnections on Ganymede's magnetopause or to some ionospheric feedback mechanism, such as the recurrent apparition of double layer structures, as documented for Io (Hess et al., 2009).

Callisto

With a faint O_2, CO_2, and H_2O atmosphere and an H corona dominated by sublimation rather than sputtering (Carlson, 1999; Cunningham et al., 2015; Roth et al., 2017), Callisto possesses a significant conductive ionosphere generated by photo-ionization (Kliore et al., 2002). A review of Callisto's atmosphere and space environment can be found in Galli et al. (2022). Signatures of an induced magnetic field, similar to Europa's, have been recorded by Galileo. It is, however, uncertain whether this induced field arises from currents in a sub-surface conductive layer (Khurana et al., 1998; Neubauer, 1998; Zimmer et al., 2000) or in the ionosphere (Hartkorn & Saur, 2017). Measurements acquired during some flybys by Galileo (namely C3 and C10) suggested the presence of a downstream plasma wake (or plume), while other (during C22) did not lead to the same conclusion (Eviatar & Paranicas, 2005; Gurnett et al., 2000). Moreover, Galileo may have encountered a field-aligned electron beam in Callisto's wake, similar to those observed at Io (Mauk & Saur, 2007). Of the four Galilean moons, Callisto is the one generating the weakest interaction, due to the lower plasma density, the weaker ambient magnetic field, and the lack of a large internal field (Saur et al., 2013). At the Jovian end of the field lines, two tentative detections of a Callisto auroral footprint were reported by Bhattacharyya et al. (2018), based on Hubble Space Telescope UV images. If the detected spots do indeed correspond to a Callisto footprint, it could be as bright as Ganymede's. However, the search for this footprint with more sensitive ultraviolet and infrared instruments on board the Juno spacecraft has been unfruitful so far (Moirano et al., 2024). In conclusion, while the signatures of the interaction similar to those observed for the other Galilean satellites are expected, their detection (of a dense wake, of electron beams, of an auroral footprint) remains uncertain, and the arrival of the JUICE spacecraft is thus much awaited.

7.2.2. The Kronian Moons

Enceladus

The moons of Saturn were not expected to trigger as strong electrodynamic interactions as those of Jupiter. Indeed, the alignment of the magnetic dipole with the rotation axis prevents oscillations of the local magnetic field at the moons to generate strong induced fields as on Jupiter's moons (only the orbital eccentricities and the local time variations would modify the local magnetic field). Moreover, the largest moon, Titan, orbits at a much larger distance from the planet, both in absolute and relative terms, than the Galilean moons. The other moons were deemed too small to hold a sub-surface ocean or even a significant ionosphere. However, the finding of a huge water ion cloud located south of Enceladus (radius: ~250 km) and originating from cryo-volcanoes led to the realization that Enceladus's environment formed a much larger obstacle than originally thought (Dougherty et al., 2006; Porco et al., 2006). Initial searches for the Enceladus auroral footprint with the Hubble Space Telescope were unsuccessful (Wannawichian et al., 2008), but later observations of the aurora from Cassini's UVIS (UltraViolet Imaging Spectrograph) demonstrated the presence of an auroral spot connected to Enceladus (Pryor et al., 2011)

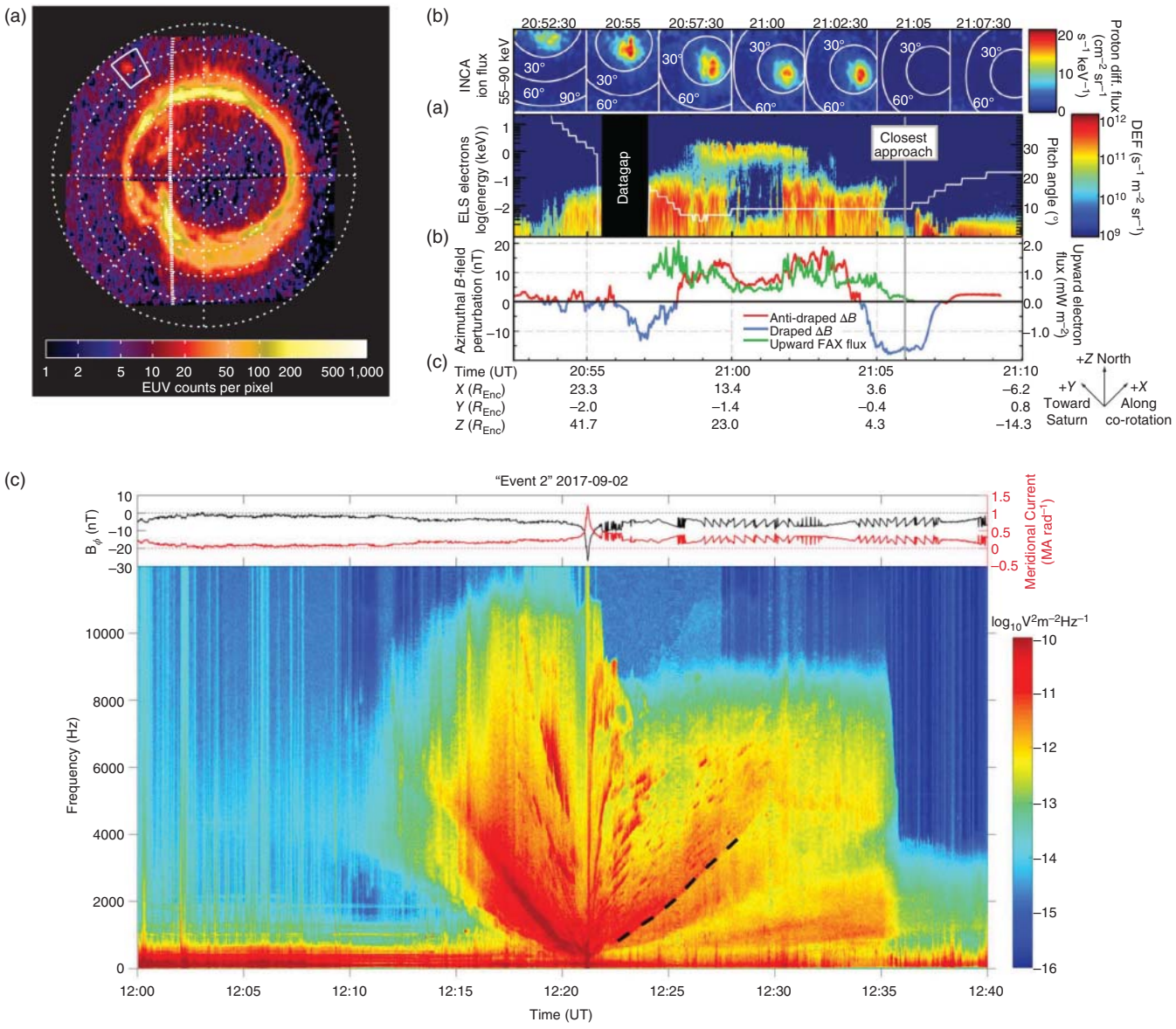

Figure 7.8 (a) Image of the Extreme-UV northern aurora at Saturn acquired on 26 August 2008 by the UltraViolet Imaging Spectrograph on board Cassini. The spot highlighted on the top left side is the Enceladus footprint. (b) Particle and field measurements acquired around 11 August 2008 flyby of Enceladus by Cassini's Ion and Neutral Camera (INCA), Electron Spectrometer (ELS), and magnetometer. The observed ion and electron beams are originating from Saturn's north pole and were thus accelerated close to the planet and away from it, reminiscent of the electron beams creating the TEB spots at Jupiter. (c) High-resolution electric field dynamic spectrogram of the auroral hiss emissions as Cassini was crossing the Enceladus Alfvén wing at high latitude on 2 September 2017. A ray-tracing analysis indicates that the source region is co-located with the Enceladus footprint on Saturn. Source: (a) and (b) are from Pryor et al. 2011 / Springer Nature, and (c) is from Sulaiman et al. (2018).

(Figure 7.8a). The electro-dynamic interaction between Enceladus and Saturn similarly gives rise to Alfvén wings (Jia et al., 2011). The location of Enceladus' plume in its southern polar region leads to a north-south asymmetry in the orientation of the Alfvén wings. Furthermore, the absorption of electrons by the dust in the plume yields a reversal of the sign of the Hall conductivity (anti-Hall effect), as well as a reversal of the sign of the B_y perturbation (i.e., the perturbation of the magnetic field along the anti-Saturn/Saturn direction) in the Alfvén wing (Kriegel et al., 2011; Simon et al., 2011). Moreover, Cassini's particle instruments detected the presence of

a field aligned ion and electron beams a few Enceladus' radii downstream of the moon. While the energy flux of these beams was sufficient to generate observable auroral footprints on Saturn, they were oriented anti-planetward, indicating that these particles had been accelerated relatively close to Saturn and away from the planet, similarly to the mechanism explaining the TEBs and their associated spots at Jupiter (see Figure 7.8b). Field-aligned currents and whistler-mode auroral hiss emissions from the beam-plasma instability have been measured near and within the Enceladus Alfvén wing (Figure 7.8c), however, unlike Io, no radio emissions have been observed (Gurnett et al., 2011; Sulaiman et al., 2018).

Titan

Titan is Saturn's largest moon (radius: 2575 km) and has a thick and hydrocarbon-rich N_2 atmosphere and a dense ionosphere, making it a significant source of plasma in Saturn's magnetosphere. However, Titan does not play the role Io plays on Jupiter, because it orbits much further away from Saturn, so that it even occasionally crosses the magnetopause. Hence, depending on its position in orbit around Saturn and on the solar wind conditions, Titan could be located either in the plasma sheet, in the magnetosphere lobes, or in the magnetosheath (Rymer et al., 2009). At such distances from the planet, the magnetic field is so weak that the plasma β is larger than 1 (Neubauer et al., 2006). In such conditions, the dynamics of the plasma (or lack thereof) takes precedence over the magnetic tension and the interacting field lines get draped around the Kronian moon. Interestingly, the timescale of convection of the magnetic field becomes longer than the timescale of the changes in the external field, and the previous magnetic field configuration thus remains "fossilized" in the thick ionosphere of Titan (Bertucci et al., 2008).

Despite the complexity of the interaction between the ever-changing magnetospheric plasma (Simon et al., 2010) and Titan's thick exosphere and ionosphere (e.g., Sillanpää et al., 2007; Snowden et al., 2013; Wei et al., 2007), numerical simulations show the systematic development of Alfvén wings connected to Titan (Kallio et al., 2007; Sillanpää & Johnson, 2015). Whether these Alfvén wings trigger any significant signature on Saturn remains to be demonstrated.

Rhea

Located in Saturn's E ring, Rhea does not have any significant magnetic field or any significant plasma source, nor is it a conducting object. Yet its surface absorbs plasma while the magnetic flux passes across the 1528 km wide moon. Close encounters with the Cassini spacecraft showed that this wake is subject to diamagnetic currents as the pressure gradients between the plasma

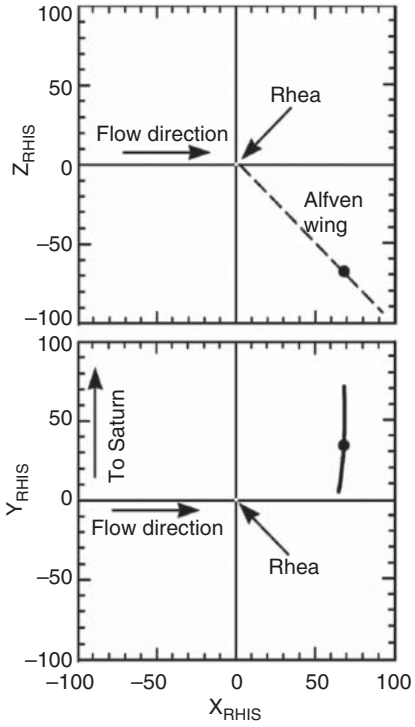

Figure 7.9 Plot of the Cassini trajectory during the distant Rhea encounter of 3 June 2010. The black circle marks the passage through the Alfvén wing. Tracing the Alfvén waves back in time (dashed lines) shows that they originate from Rhea or its close wake. Source: Khurana et al., 2017 / John Wiley & Sons.

void (~4-6 R_{Rh} long) and the surrounding plasma distorts and bends the field lines, generating Alfvén waves (Simon et al., 2012). Furthermore, a more distant flyby (102 R_{Rh}, see Figure 7.9) revealed that the Alfvén wings were still present far away from Rhea and that the associated currents probably close in Saturn's ionosphere (Khurana et al., 2017). Khurana et al. (2017) also argue that it is the deceleration of the plasma in the wake resulting from the pressure gradient rather than the diamagnetic currents themselves that generate most of the Alfvénic disturbance.

7.2.3. Triton

The time variability of Neptune's magnetic field that is intercepted by Triton is especially large due to the tilt between Neptune's magnetic and rotational axes, as well as Triton's large orbital obliquity. The resulting structure of the electro-dynamic interaction is highly asymmetric, with one of Triton's Alfvén wings shown to be oriented toward upstream, initiating the deflection of the incident flow farther than it would otherwise (Simon et al., 2022). It is, therefore, reasonable to expect a highly complex current system and propagation pattern of Alfvén waves,

and, consequently, regions where dissipation, particle acceleration, and auroral generation would take place.

7.2.4. The Earth

At 1 astronomical unit (AU), the solar wind's Alfvén Mach number is generally on the order of 8, thus the conditions are not favorable to the formation of significant Alfvén wings, as they bend over to form the magnetotail lobes (see the top left panel in Figure 7.1). However, during the passage of an interplanetary coronal mass ejection (ICME) across the Earth, the density of the solar wind can occasionally become so low and the field strength so high that the interaction gets both sub-fast and sub-Alfvénic. Under such atypical conditions, magneto-hydrodynamic simulations show that the bow shock expands out and vanishes, and well-formed Alfvén wings develop (Ridley, 2007) (see Figure 7.1). Chané et al. (2012) found observational evidence that the Earth entered into such a regime for four hours between 24 and 25 May 2002. During this interval, the magnetic field wasn't unusually high (~9.8 nT), but the estimated density dropped down to 0.05 cm^{-3} (compared to typical values between 0.6 and 20 cm^{-3}). The Geotail spacecraft was located on the dusk side of the Earth and its magnetic field and plasma velocity measurements suggest that the spacecraft entered and exited the Alfvén wing nine times. Figure 7.10 shows the expected shape and orientation of the Alfvén wings during this time interval compared to the typical shape of the terrestrial magnetosphere. Such exceptionally low density values were achieved because an ICME expanded right in the wake of another one (Chané et al., 2021).

The Moon

The Moon is also an inert object without any significant magnetic field or mass-loading source. Moreover, the Moon orbits so far away from the Earth that it spends most of its time in the supersonic and super Alfvénic interplanetary medium. And yet, the two Moon orbiting ARTEMIS spacecrafts found a bending of the magnetic field and a deceleration of the plasma flow in the Moon's wake, which are interpreted as characteristic signatures of Alfvén waves (Zhang et al., 2016) (see Figure 7.11). It is, however, unlikely that this configuration would allow a significant amount of energy and current to propagate along the magnetic field lines.

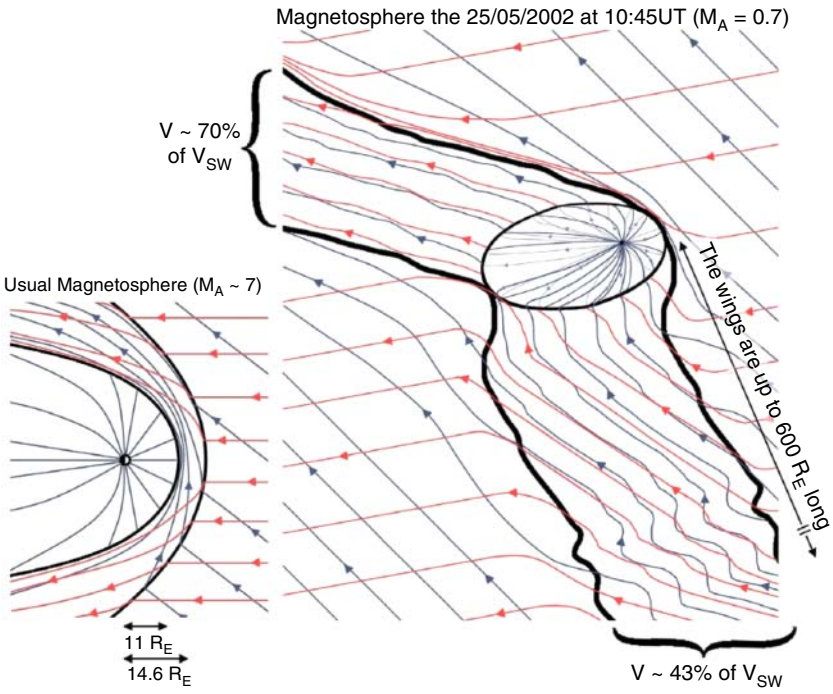

Figure 7.10 Sketches of the interaction between the solar wind and the Earth's magnetosphere seen from the north. The magnetic field is shown in blue, the velocity in red. The left sketch shows the typical configuration of the magnetosphere while the right one shows the development of Alfvén wings at a time during which the interplanetary medium density at Earth dropped so much that the Alfvén Mach number was below one. The Geotail spacecraft was located on the dusk side of the Earth (i.e., toward the top of the image) and entered and exited from the Alfvén wing several times. Source: Chané et al. (2012) / John Wiley & Sons.

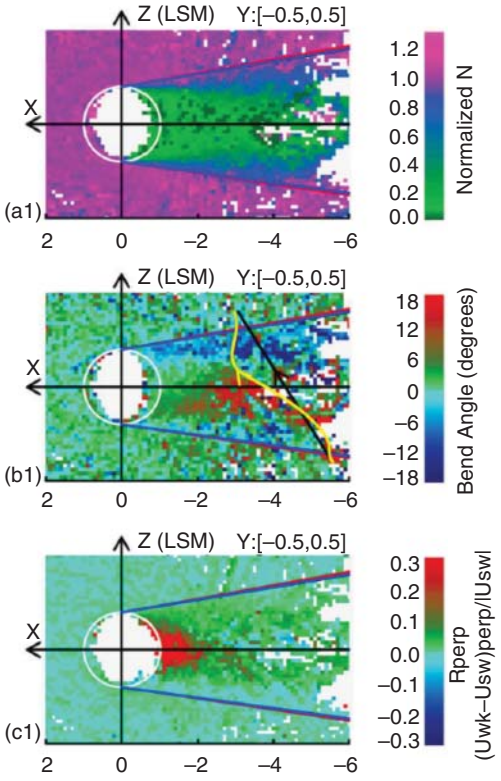

Figure 7.11 Distribution of the average ARTEMIS measurements for the density normalized by the ion density in the solar wind (top), the bent angle of the magnetic field magnetic δ_{XZ} (middle), and the X component of the plasma flow deceleration rate in the Moon's wake (bottom). The density gradient stemming from the absorption of the plasma by th Moon's surface is the source of Alfvén wings, which manifest through a deceleration of the plasma flow and a bending of the magnetic field in the wake. Source: Zhang et al. (2016) / John Wiley & Sons.

7.2.5. Mercury

Since Mercury is closer to the Sun than the Earth (perihelion:0.31 AU and aphelion:0.47 AU), the typical magnetic field strength, and thus the typical Alfvén Mach number is also much lower than for the Earth (~2–3 compared to ~8 or above for the Earth). Hence, Alfvén Mach number excursions below 1 during ICME crossings are also expected to be more frequent, especially throughout the time intervals for which the field is strong, but the density is low after the initial interplanetary shock. Using a simple analytical models, Sarantos and Slavin (2009) explored the possibility for the formation of Alfvén wings at Mercury with a low Alfvén Mach number, since Mercury, under such configurations, is expected to be an intermediate state between Ganymede and the Earth. The BepiColombo mission may soon bring us further evidence of Alfvén wings originating from Mercury.

7.2.6. Exoplanets

As discussed before, the interaction between Solar System planets and the solar wind can occasionally become sub-Alfvénic, allowing for the propagation of energy at large distances. However, even at Mercury, the Alfvén speed remains lower than the solar wind speed, and these waves will never reach the solar atmosphere. Indeed, the Alfvén radius, i.e., the limit inside which the Alfvén speed is larger than the stellar wind speed, is $\lesssim$0.1 AU while Mercury orbits at least three times farther out. However, an increasingly large number of exoplanets are being discovered, and many of them orbit at close distances relative to their parent stars, including some orbiting inside the Alfvén radius, making it possible to trigger a planetary footprint on the star. Furthermore, observational evidences are accumulating in favor of such a Star Planet Magnetic Interaction (SPMI). These evidences can be sorted into two categories: one focuses on single targets and requires the monitoring of a star's luminosity through time, and the second consists of statistical investigations of anomalous stellar activity on large catalogs of stars with known close-in exoplanets. In the first category, the most compelling case probably concerns HD 179949, which shows a surplus of Ca II K chromospheric emissions which is synchronous with the orbital period of a known exoplanet (Shkolnik et al., 2003). Other tentative evidences were reported based on optical broadband photometry (Pagano et al., 2009; Walker et al., 2008) or X-ray emissions (Maggio et al., 2015). Unfortunately, the statistical approach has not provided conclusive evidence yet (e.g., Viswanath et al., 2020).

It should be noted that the electro–magnetic interaction between planets and stars may be much more varied and complex than those studied in our Solar System. For example, the relative motion of the planet in the plasma stream is most often dominated by the radial motion of the stellar wind rather than the orbital motion of the planet. Moreover, while the orientation of the stellar magnetic field may be mostly latitudinal for a planet orbiting very close; it is expected to become essentially longitudinal at larger distances. Then the planets and their magnetospheres may also display more varied configurations (presence of conductive layers, atmospheres, ionospheres and magnetospheres) compared to the moons of the Giant Planets. And finally, the star's intrinsic variability and activity certainly complicate the picture and probably explains why SPMI signatures are not systematically observed, even at HD 179949 (Shkolnik et al., 2008). But the most important argument to consider is the fact that a stellar atmosphere is quite different than a planetary one. Indeed some authors have noted that the power of the excess chromospheric emissions appeared

three orders of magnitude larger than the expected energy arising from the Alfvénic interaction (Saur et al., 2013). This finding motivated the investigation of alternative scenarios, where the SPMI would modulate the star's emissions rather than directly providing the energy. The interested reader is referred to the recent reviews by Shkolnik and Llama (2018); Saur (2018); and Strugarek (2018).

7.3. SUMMARY

The electro–dynamic interaction between a plasma flow and large celestial bodies, especially at a low Alfvén Mach number, can generate powerful Alfvén waves propagating energy at large distances along the magnetic field lines. But the Alfvén waves generation is only the first step of a long chain of processes, including turbulence, complex reflection patterns, electric currents, energy transport and dissipation, momentum transfer, wave–particle interaction, aurora, joule heating of the ionosphere of the parent planet, and powerful radio emission. Examples of similar interactions abound in the Solar System, but the Jovian moons and the Io–Jupiter interaction in particular, are the best studied ones so far. Indeed, this case benefits both from a low Alfvén Mach number, strong energy generation, and relative stability of the incoming plasma characteristics, which all facilitate the measurements of the signatures of the Alfvén waves and their consequences, as well as their interpretation. For other systems, the puzzle is missing more pieces, as sometimes we only have access to hints of the local interaction. It is, however, remarkable that Alfvén wings have been observed for bodies as diverse as Rhea, Io, Europa, Ganymede, or the Earth. Electron beams, most probably accelerated by Alfvén waves, have been observed at Io, Ganymede, Callisto, and Enceladus, while auroral footprints have been reported for all four Galilean moons and for Enceladus. Despite the idiosyncrasies associated with each individual moon or planet, general patterns emerge and similar processes are observed, indicating that such processes are universal and probably very common in the universe. With missions specifically dedicated to the Galilean moons, such as JUICE and Europa Clipper, the BebiColombo mission arriving at Mercury or a future mission dedicated to the exploration of the Ice Giants, we can expect that the next decades will bring us a wealth of observational clues to further complete our understanding of the way Alfvén waves mediate the interaction between celestial objects and the plasma flows surrounding them. Even beyond the limits of our Solar System, evidences are starting to emerge, showing the importance of the Alfvén waves in the interaction between planets and their parent stars.

REFERENCES

Acuña, M. H., Neubauer, F. M., & Ness, N. F. (1981). Standing Alfvén wave current system at Io: Voyager 1 observations. *Journal of Geophysical Research: Space Physics*, *86*(A10), 8513–8521. ISSN 2156-2202. doi: 10.1029/JA086iA10p08513.

Allegrini, F., Gladstone, G. R., Hue, V., Clark, G., Szalay, J. R., Kurth, W. S., et al. (2020). First report of electron measurements during a Europa Footprint Tail Crossing by Juno. *Geophysical Research Letters*, *47*(18), e2020GL089732. ISSN 1944-8007. doi: 10.1029/2020GL089732.

Arnold, H., Liuzzo, L., & Simon, S. (2019). Magnetic Signatures of a Plume at Europa During the Galileo E26 Flyby. *Geophysical Research Letters*, *46* (3), 1149–1157. ISSN 1944-8007. doi: 10.1029/2018GL081544.

Bagenal, F. (1983). Alfvén wave propagation in the Io plasma torus. *Journal of Geophysical Research: Space Physics*, *88*(A4), 3013–3025. ISSN 2156-2202. doi: 10.1029/JA088iA04p03013.

Bagenal, F., & Dols, V. (2020). The Space Environment of Io and Europa. *Journal of Geophysical Research: Space Physics*, *125*(5), e2019JA027485. ISSN 2169-9402. doi: 10.1029/2019JA027485.

Belcher, J. W., Goertz, C. K., Sullivan, J. D., & Acunã, M. H. (1981). Plasma observations of the Alfvén wave generated by Io. *Journal of Geophysical Research: Space Physics*, *86*(A10), 8508–8512. ISSN 2156-2202. doi: 10.1029/JA086iA10p08508.

Bertucci, C., Achilleos, N., Dougherty, M. K., Modolo, R., A. Coates, J., Szego, K., et al. (2008). The Magnetic Memory of Titan's Ionized Atmosphere. *Science*, *321*(5895), 1475–1478. doi: 10.1126/science.1159780. Publisher: American Association for the Advancement of Science.

Bhattacharyya, D., Clarke, J. T., Montgomery, J., Bonfond, B., Gérard, J.-C., & Grodent, D. (2018). Evidence for auroral emissions From Callisto's footprint in HST UV Images. *Journal of Geophysical Research: Space Physics*, *123*(1), 364–373. ISSN 2169-9402. doi: 10.1002/2017JA024791.

Bigg, E. K. (1964). Influence of the satellite Io on Jupiter's decametric emission. *Nature*, *203*(4949), 1008–1010. ISSN 1476-4687. doi: 10.1038/2031008a0.

Blöcker, A., Saur, J., & Roth, L. (2016). Europa's plasma interaction with an inhomogeneous atmosphere: Development of Alfvén winglets within the Alfvén wings. *Journal of Geophysical Research: Space Physics*, *121* (10), 9794–9828. ISSN 2169-9402. doi: 10.1002/2016JA022479.

Bonfond, B. (2010). The 3-D extent of the Io UV footprint on Jupiter. *Journal of Geophysical Research: Space Physics*, *115*(A9), A09217. ISSN 2156-2202. doi: 10.1029/2010JA015475.

Bonfond, B. (2012). When Moons Create Aurora: The Satellite Footprints on Giant Planets. In *Geophysical Monograph Series*. AGU. ISBN 978-0-87590-487-0. doi: 10.1029/2011GM001169.

Bonfond, B., Gérard, J.-C., Grodent, D., & Saur, J. (2007). Ultraviolet Io footprint short timescale dynamics. *Geophysical Research Letters*, *34* (6). ISSN 1944-8007. doi: 10.1029/2006GL028765.

Bonfond, B., Grodent, D., Gérard, J.-C., Radioti, A., Saur, J., & Jacobsen, S. (2008). UV Io footprint leading spot: A key feature for understanding the UV Io footprint multiplicity?

Geophysical Research Letters, *35*(5). ISSN 1944-8007. doi: 10.1029/2007GL032418.

Bonfond, B., Grodent, D., Gérard, J.-C., Radioti, A., Dols, V., Delamere, P. A., & Clarke, J. T. (2009). The Io UV footprint: Location, inter-spot distances and tail vertical extent. *Journal of Geophysical Research: Space Physics*, *114*(A7). ISSN 2156-2202. doi: 10.1029/2009JA014312.

Bonfond, B., Grodent, D., Gérard, J.-C., Stallard, T., Clarke, J. T., Yoneda, M., et al. (2012). Auroral evidence of Io's control over the magnetosphere of Jupiter. *Geophysical Research Letters*, *39*(1), L01105. ISSN 1944-8007. doi: 10.1029/2011GL050253.

Bonfond, B., Hess, S., Bagenal, F., Gérard, J.-C., Grodent, D., Radioti, A., et al. (2013). The multiple spots of the Ganymede auroral footprint. *Geophysical Research Letters*, *40*(19), 4977–4981. ISSN 1944-8007. doi: 10.1002/grl.50989.

Bonfond, B., Hess, S., Gérard, J. C., Grodent, D., Radioti, A., Chantry, V., et al. (2013). Evolution of the Io footprint brightness I: Far-UV observations. *Planetary and Space Science*, *88*, 64–75. ISSN 0032-0633. doi: 10.1016/j.pss.2013.05.023.

Bonfond, B., Grodent, D., Badman, S. V., Saur, J., Gérard, J. C., & Radioti, A. (2017). Similarity of the Jovian satellite footprints: Spots multiplicity and dynamics. *Icarus*, *292*, 208–217. ISSN 0019-1035. doi: 10.1016/j.icarus.2017.01.009.

Bonfond, B., Saur, J., Grodent, D., Badman, S. V., Bisikalo, D., Shematovich, V., et al. (2017). The tails of the satellite auroral footprints at Jupiter. *Journal of Geophysical Research: Space Physics*, *122*(8), 7985–7996. ISSN 2169-9402. doi: 10.1002/2017JA024370.

Bonfond, B., Yao, Z., & Grodent, D. (2020). Six observational pieces of evidence against corotation as the main cause for the aurora at Jupiter. Copernicus Meetings. doi: https://doi.org/10.5194/epsc2020-29.

Carlson, R. W. (1999). A tenuous carbon dioxide atmosphere on Jupiter's Moon Callisto. *Science*, *283*(5403), 820–821. doi: 10.1126/science.283.5403.820.

Chané, E., Saur, J., Neubauer, F. M., Raeder, J., & Poedts, S. (2012). Observational evidence of Alfvén wings at the Earth. *Journal of Geophysical Research: Space Physics*, *117*(A9). ISSN 2156-2202. doi: 10.1029/2012JA017628.

Chané, E., Schmieder, B., Dasso, S., Verbeke, C., Grison, B., Démoulin, P., & Poedts, S. (2021). Over-expansion of a coronal mass ejection generates sub-Alfvénic plasma conditions in the solar wind at Earth. *Astronomy & Astrophysics*, *647*, A149. ISSN 0004-6361, 1432-0746. doi: 10.1051/0004-6361/202039867. Publisher: EDP Sciences.

Cheng, A. F., & Paranicas, C. (1998). Model of field aligned potential drops near Io. *Geophysical Research Letters*, *25*(6), 833–836. ISSN 1944-8007. doi: 10.1029/98GL00407.

Chust, T., Roux, A., Kurth, W. S., Gurnett, D. A., Kivel son, M. G., & Khurana, K. K. (2005). Are Io's Alfvén wings filamented? Galileo observations. *Planetary and Space Science*, *53*(4), 395–412. ISSN 0032-0633. doi: 10.1016/j.pss.2004.09.021.

Clark, G., Mauk, B. H., Kollmann, P., Szalay, J. R., Sulaiman, A. H., Gershman, D. J., et al. (2020). Energetic proton acceleration associated with Io's footprint tail. *Geophysical Research Letters*, *47*(24), e2020GL090839. ISSN 1944-8007. doi: 10.1029/2020GL090839.

Clarke, J. T., Ballester, G. E., Trauger, J., Evans, R., Connerney, J. E. P., Stapelfeldt, K., et al. (1996). Far-Ultraviolet Imaging of Jupiter's Aurora and the Io "Footprint". *Science*, *274*(5286), 404–409, Oct. 1996. ISSN 0036-8075, 1095-9203. doi: 10.1126/science.274.5286.404.

Clarke, J. T., Ajello, J., Ballester, G., Jaffel, L. B., Connerney, J., Gérard, J.-C., et al. (2002). Ultraviolet emissions from the magnetic footprints of Io, Ganymede and Europa on Jupiter. *Nature*, *415* (6875), 997–1000. ISSN 1476-4687. doi: 10.1038/415997a.

Connerney, J. E. P., Baron, R., Satoh, T., & Owen, T. (1993). Images of Excited H_3^+ at the Foot of the lo Flux Tube in Jupiter's Atmosphere. *Science*, *262*(5136), 1035–1038. ISSN 0036-8075, 1095-9203. doi: 10.1126/science.262.5136.1035.

Crary, F. J. (1997). On the generation of an electron beam by Io. *Journal of Geophysical Research: Space Physics*, *102*(A1), 37–49. ISSN 2156-2202. doi: 10.1029/96JA02409.

Crary, F. J., & Bagenal, F. (1997). Coupling the plasma interaction at Io to Jupiter. *Geophysical Research Letters*, *24*(17), 2135–2138. ISSN 1944-8007. doi: 10.1029/97GL02248.

Cunningham, N. J., Spencer, J. R., Feldman, P. D., Strobel, D. F., France, K., & Osterman, S. N. (2015). Detection of Callisto's oxygen atmosphere with the Hubble Space Telescope. *Icarus*, *254*, 178–189. ISSN 0019-1035. doi: 10.1016/j.icarus.2015.03.021.

Damiano, P. A., Delamere, P. A., Stauffer, B., Ng, C.-S., & Johnson, J. R. (2019). Kinetic simulations of electron acceleration by dispersive scale Alfvén waves in Jupiter's magnetosphere. *Geophysical Research Letters*, *46* (6), 3043–3051. ISSN 1944-8007. doi: 10.1029/2018GL081219.

Delamere, P. A., Bagenal, F., Ergun, R., & Su, Y.-J. (2003). Momentum transfer between the Io plasma wake and Jupiter's ionosphere. *Journal of Geophysical Research: Space Physics*, *108*(A6), 1241. ISSN 2156-2202. doi: 10.1029/2002JA009530

Dougherty, M. K., Khurana, K. K., Neubauer, F. M., Russell, C. T., Saur, J., Leisner, J. S., & Burton, M. E. (2006). Identification of a dynamic atmosphere at Enceladus with the Cassini magnetometer. *Science*, *311*(5766), 1406–1409. doi: 10.1126/science.1120985.

Drell, S. D., Foley, H. M., & Ruderman, M. A. (1965). Drag and propulsion of large satellites in the ionosphere: An Alfvén propulsion engine in space. *Journal of Geophysical Research (1896-1977)*, *70*(13), 3131–3145. ISSN 2156-2202. doi: 10.1029/JZ070i013p03131.

Ergun, R. E., Ray, L., Delamere, P. A., Bagenal, F., Dols, V., & Su, Y.-J. (2009). Generation of parallel electric fields in the Jupiter–Io torus wake region. *J. Geophys. Res.*, *114*, A05201 doi: 10.1029/2008JA013968.

Eviatar, A., & Paranicas, C. (2005). The plasma plumes of Europa and Callisto. *Icarus*, *178*(2), 360–366. ISSN 0019-1035. doi: 10.1016/j.icarus.2005.06.007.

Eviatar, A., Williams, D. J., Paranicas, C., McEntire, R. W., Mauk, B. H., & Kivelson, M. G. (2000). Plasma flow in the magnetosphere of Ganymede. *Geophysical Research Letters*, *25*(8), 1257–1260, 1998. ISSN 1944-8007. doi: 10.1029/98GL50867.

Eviatar, A., Williams, D. J., Paranicas, C., McEntire, R. W., Mauk, B. H., & Kivelson, M. G. (2000). Trapped energetic electrons in the magnetosphere of Ganymede. *Journal of Geophysical Research: Space Physics*, *105*(A3), 5547–5553. ISSN 2156-2202. doi: 10.1029/1999JA900450.

Frank, L. A., & Paterson, W. R. (1999). Intense electron beams observed at Io with the Galileo spacecraft. *Journal of Geophysical Research: Space Physics*, *104*(A12), 28657–28669. ISSN 2156-2202. doi: 10.1029/1999JA900402.

Frank, L. A., Paterson, W. R., Ackerson, K. L., Vasyliunas, V. M., Coroniti, F. V., & Bolton, S. J. (1996). Plasma Observations at Io with the Galileo Spacecraft. *Science*, *274*(5286), 394–395. ISSN 0036-8075, 1095-9203. doi: 10.1126/science.274.5286.394.

Frank, L. A., Paterson, W. R., Ackerson, K. L., & Bolton, S. J. (1997). Low-energy electron measurements at Ganymede with the Galileo spacecraft: Probes of the magnetic topology. *Geophysical Research Letters*, *24*(17), 2159–2162. ISSN 1944-8007. doi: 10.1029/97GL01632.

Galli, A., Vorburger, A., Carberry Mogan, S. R., Roussos, E., Stenberg, G., Wieser, Wurz, P., et al. (2022). Callisto's atmosphere and its space environment: Prospects for the particle environment package on board JUICE. *Earth and Space Science*, *9*(5), e2021EA002172. ISSN 2333-5084. doi: 10.1029/2021EA002172.

Gershman, D. J., Connerney, J. E. P., Kotsiaros, S., DiBraccio, G. A., Martos, Y. M., -Vinãs, A. F., et al. (2019). Alfvénic fluctuations associated With Jupiter's auroral emissions. *Geophysical Research Letters*, *46*(13), 7157–7165. ISSN 1944-8007. doi: 10.1029/2019GL082951.

Gladstone, G. R., Stern, S. A., Slater, D. C., Versteeg, M., Davis, M. W., Retherford, K. D., et al. (2007). Jupiter's Nightside Airglow and Aurora. *Science*, *318*(5848), 229–231. ISSN 0036-8075, 1095-9203. doi: 10.1126/science.1147613.

Goertz, C. (1980). Io's interaction with the plasma torus. *Journal of Geophysical Research: Space Physics*, *85*(A6), 2949–2956. ISSN 2156-2202. doi: 10.1029/JA085iA06p02949.

Goldreich, P., & Lynden-Bell, D. (1969). Io, a jovian unipolar inductor. *Astrophysical Journal*, *156*, 59–78.

Grodent, D., Gérard, J.-C., Gustin, J., Mauk, B. H., Connerney, J. E. P., & Clarke, J. T. (2006). Europa's FUV auroral tail on Jupiter. *Geophysical Research Letters*, *33*, 6201–+. doi: 10.1029/2005GL025487.

Grodent, D., Bonfond, B., Radioti, A., Gérard, J.-C., Jia, X., Nichols, J. D., & Clarke, J. T. (2009). Auroral footprint of Ganymede. *Journal of Geophysical Research: Space Physics*, *114*(A7), A07212. ISSN 2156-2202. doi: 10.1029/2009JA014289.

Gurnett, D. A., & Goertz, C. K. (1981). Multiple Alfven wave reflections excited by Io: Origin of the Jovian decametric arcs. *Journal of Geophysical Research: Space Physics*, *86*(A2), 717–722. ISSN 2156-2202. doi: 10.1029/JA086iA02p00717.

Gurnett, D. A., Kurth, W. S., Roux, A., Bolton, S. J., & Kennel, C. F. (1996). Evidence for a magnetosphere at Ganymede from plasma-wave observations by the Galileo spacecraft. *Nature*, *384* (6609), 535–537. ISSN 1476-4687. doi: 10.1038/384535a0. Number: 6609 Publisher: Nature Publishing Group.

Gurnett, D. A., Persoon, A. M., Kurth, W. S., Roux, A., & Bolton, S. J. (2000). Plasma densities in the vicinity of Callisto from Galileo plasma wave observations. *Geophysical Research Letters*, *27*(13), 1867–1870. ISSN 1944-8007. doi: 10.1029/2000GL003751.

Gurnett, D. A., Averkamp, T. F., Schippers, P., Persoon, A. M., Hospodarsky, G. B., Leisner, J. S., et al. (2011). Auroral hiss, electron beams and standing Alfvén wave currents near Saturn's moon Enceladus. *Geophysical Research Letters*, *38*(6), L06102. ISSN 1944-8007. doi: 10.1029/2011GL046854.

Gérard, J.-C., Saglam, A., Grodent, D., & Clarke, J. T. (2006). Morphology of the ultraviolet Io footprint emission and its control by Io's location. *Journal of Geophysical Research*, *111*(A10), 4202–+. doi: 10.1029/2005JA011327.

Hartkorn, O., & Saur, J. (2017). Induction signals from Callisto's ionosphere and their implications on a possible subsurface ocean. *Journal of Geophysical Research: Space Physics*, *122*(11), 11,677–11,697. ISSN 2169-9402. doi: 10.1002/2017JA024269.

Hess, S., Zarka, P., Mottez, F., & Ryabov, V. B. (2009). Electric potential jumps in the Io-Jupiter flux tube. *Planetary and Space Science*, *57*(1), 23–33. ISSN 0032-0633. doi: 10.1016/j.pss.2008.10.006.

Hess, S. L. G., Delamere, P., Dols, V., Bonfond, B., & Swift, D. (2010). Power transmission and particle acceleration along the Io flux tube. *Journal of Geophysical Research: Space Physics*, *115*(A6), 23–33. ISSN 2156-2202. doi: 10.1029/2009JA014928.

Hess, S. L. G., Delamere, P., Dols, A. V., & Ray, L. C. (2011). Comparative study of the power transferred from satellite-magnetosphere interactions to auroral emissions. *Journal of Geophysical Research: Space Physics*, *116*(A1), A01202. ISSN 2156-2202. doi: 10.1029/2010JA015807.

Hess, S. L. G., Bonfond, B., Chantry, V., Gérard, J. C., Grodent, D., Jacobsen, S., & Radioti, A. (2013). Evolution of the Io footprint brightness II: Modeling. *Planetary and Space Science*, *88*, 76–85. ISSN 0032-0633. doi: 10.1016/j.pss.2013.08.005.

Hess, S. L. G., Bonfond, B., & Delamere, P. A. (2013). How could the Io footprint disappear? *Planetary and Space Science*, *89*, 102–110. ISSN 0032-0633. doi: 10.1016/j.pss.2013.08.014.

Hill, T. W., & Vasyliūnas, V. M. (2002). Jovian auroral signature of Io's corotational wake. *Journal of Geophysical Research: Space Physics*, *107*(A12), SMP 27–1–SMP 27–5. ISSN 2156-2202. doi: 10.1029/2002JA009514.

Hinson, D. P., Kliore, A. J., Flasar, F. M., Twicken, J. D., Schinder, P. J., & Herrera, R. G. (1998). Galileo radio occultation measurements of Io's ionosphere and plasma wake. *Journal of Geophysical Research*, *103*, 29343–29358. doi: 10.1029/98JA02659.

Hinton, P. C., Bagenal, F., & Bonfond, B. (2019). Alfvén wave propagation in the Io Plasma Torus. *Geophysical Research Letters*, *46*(3), 1242–1249. ISSN 1944-8007. doi: 10.1029/2018GL081472.

Hue, V., Greathouse, T. K., Bonfond, B., Saur, J., Gladstone, G. R., Roth, L. (2019). Juno-UVS observation of the Io footprint during solar eclipse. *Journal of Geophysical Research: Space Physics*, *124*(7), 5184–5199. ISSN 2169-9402. doi: 10.1029/2018JA026431.

Hue, V., Greathouse, T. K., Gladstone, G. R., Bonfond, B., Gérard, J.-C., Vogt, M. F., et al. (2021). Detection and characterization of circular expanding UV-emissions observed in Jupiter's Polar Auroral regions. *Journal of Geophysical Research: Space Physics*, *126*(3), e2020JA028971. ISSN 2169-9402. doi: 10.1029/2020JA028971.

Huybrighs, H. L. F., Roussos, E., Blöcker, A., Krupp, N., Futaana, Y., Barabash, S., et al. (2020). An active plume eruption on europa During Galileo Flyby E26 as indicated by energetic Proton depletions. *Geophysical Research Letters*, *47*(10), e2020GL087806. ISSN 1944-8007. doi: 10.1029/2020GL087806.

Jacobsen, S., Saur, J., Neubauer, F. M., Bonfond, B., Gérard, J.-C., & Grodent, D. (2010). Location and spatial shape of electron beams in Io's wake. *Journal of Geophysical Research*, *115*(A14), A04205. doi: 10.1029/2009JA014753.

Jia, X., Walker, R. J., Kivelson, M. G., Khurana, K. K., & Linker, J. A. (2008). Three-dimensional MHD simulations of Ganymede's magnetosphere. *Journal of Geophysical Research*, *113*(A12), 6212–+. doi: 10.1029/2007JA012748.

Jia, X., Kivelson, M. G., Khurana, K. K., & Kurth, W. S. (2018). Evidence of a plume on Europa from Galileo magnetic and plasma wave signatures. *Nature Astronomy*, *2*(6), 459–464. ISSN 2397-3366. doi: 10.1038/s41550-018-0450-z.

Jia, Y.-D., Russell, C. T., Khurana, K. K., Wei, H. Y., Ma, Y. J., Leisner, J. S., et al. (2011). Cassini magnetometer observations over the Enceladus poles. *Geophysical Research Letters*, *38*(19). ISSN 1944-8007. doi: 10.1029/2011GL049013.

Jones, S. T., & Su, Y.-J. (2008). Role of dispersive Alfvén waves in generating parallel electric fields along the Io-Jupiter fluxtube. *Journal of Geophysical Research*, *113*(A12), 12205–+. doi: 10.1029/2008JA013512.

Kallio, E., Sillanpää, I., Jarvinen, R., Janhunen, P., Dougherty, M., Bertucci, C., & Neubauer, F. (2007). Morphology of the magnetic field near Titan: Hybrid model study of the Cassini T9 flyby. *Geophysical Research Letters*, *34*(24). ISSN 1944-8007. doi: 10.1029/2007GL030827.

Khurana, K. K., Kivelson, M. G., Stevenson, D. J., Schubert, G., Russell, C. T., Walker, R. J., & Polanskey, C. (1998). Induced magnetic fields as evidence for subsurface oceans in Europa and Callisto. *Nature*, *395*(6704), 777–780. ISSN 1476-4687. doi: 10.1038/27394.

Khurana, K. K., Fatemi, S., Lindkvist, J., Roussos, E., Krupp, N., Holmström, M., et al. (2017). The role of plasma slowdown in the generation of Rhea's Alfvén wings. *Journal of Geophysical Research: Space Physics*, *122*(2), 1778–1788. ISSN 2169-9402. doi: 10.1002/2016JA023595.

Kivelson, M. G., Khurana, K. K., Walker, R. J., Russell, C. T., Linker, J. A., Southwood, D. J., & Polanskey, C. (1996). A Magnetic Signature at Io: Initial Report from the Galileo Magnetometer. *Science*, *273*(5273), 337–340. doi: 10.1126/science.273.5273.337. Publisher: American Association for the Advancement of Science.

Kivelson, M. G., Warnecke, J., Bennett, L., Joy, S., Khurana, K. K., Linker, J. A., et al. (1998). Ganymede's magnetosphere: Magnetometer overview. *Journal of Geophysical Research: Planets*, *103*(E9), 19963–19972. ISSN 2156-2202. doi: 10.1029/98JE00227.

Kivelson, M. G., Khurana, K. K., Stevenson, D. J., Bennett, L., Joy, S., Russell, C. T., et al. (1999). Europa and Callisto: Induced or intrinsic fields in a periodically varying plasma environment. *Journal of Geophysical Research*, *104*, 4609–4626. doi: 10.1029/1998JA900095.

Kivelson, M. G., Khurana, K. K., Russell, C. T., Volwerk, M., Walker, R. J., & Zimmer, C. (2000). Galileo Magnetometer Measurements: A Stronger Case for a Subsurface Ocean at Europa. *Science*, *289*(5483), 1340–1343. doi: 10.1126/science.289.5483.1340. Publisher: American Association for the Advancement of Science.

Kivelson, M. G., Bagenal, F., Kurth, W. S., Neubauer, F. M., Paranicas, C., & Saur, J. (2004). Magnetospheric interactions with satellites. Jupiter: The Planet, Satellites and Magnetosphere (pages 513–536).

Kliore, A. J., Fjeldbo, G., Seidel, B. L., Sweetnam, D. N., Sesplaukis, T. T., Woiceshyn, P. M., & Rasool, S. I. (1975). The atmosphere of Io from Pioneer 10 radio occultation measurements. *Icarus*, *24*(4), 407–410. ISSN 0019-1035. doi: 10.1016/0019-1035(75)90057-3.

Kliore, A. J., Anabtawi, A., Herrera, R. G., Asmar, S. W., Nagy, A. F., Hinson, D. P., & Flasar, F. M. (2002). Ionosphere of Callisto from Galileo radio occultation observations. *Journal of Geophysical Research: Space Physics*, *107*(A11), SIA 19–1–SIA 19–7. ISSN 2156-2202. doi: 10.1029/2002JA009365.

Kriegel, H., Simon, S., Motschmann, U., Saur, J., Neubauer, F. M., Persoon, A. M., et al. (2011). Influence of negatively charged plume grains on the structure of Enceladus' Alfvén wings: Hybrid simulations versus Cassini Magnetometer data. *Journal of Geophysical Research: Space Physics*, *116*(A10), A10223. ISSN 2156-2202. doi: 10.1029/2011JA016842.

Kurth, W. S., Gurnett, D. A., Persoon, A. M., Roux, A., Bolton, S. J., & Alexander, C. J. (2001). The plasma wave environment of Europa. *Planetary and Space Science*, *49*(3), 345–363. ISSN 0032-0633. doi: 10.1016/S0032-0633(00)00156-2.

Lavrukhin, A. S., & Alexeev, I. I. (2015). Aurora at high latitudes of Ganymede. *Astronomy Letters*, *41*(11), 687–692. ISSN 1562-6873. doi: 10.1134/S1063773715110043.

Louis, C. K., Lamy, L., Zarka, P., Cecconi, B., & Hess, S. L. G. (2017). Detection of Jupiter decametric emissions controlled by Europa and Ganymede with Voyager/PRA and Cassini/RPWS. *Journal of Geophysical Research: Space Physics*, *122*(9), 9228–9247. ISSN 2169-9402. doi: 10.1002/2016JA023779.

Louis, C. K., Lamy, L., Zarka, P., Cecconi, B., Imai, M., Kurth, W. S., et al. (2017). Io-Jupiter decametric arcs observed by Juno/Waves compared to ExPRES simulations. *Geophysical Research Letters*, *44*(18), 9225–9232. ISSN 1944-8007. doi: 10.1002/2017GL073036.

Louis, C. K., Louarn, P., Allegrini, F., Kurth, W. S., & Szalay, J. R. (2020). Ganymede-Induced Decametric Radio Emission: In Situ Observations and Measurements by Juno. *Geophysical Research Letters*, *47*(20), e2020GL090021. ISSN 1944-8007. doi: https://doi.org/10.1029/2020GL090021.

Lysak, R. L. (2023). Kinetic Alfvén waves and auroral particle acceleration: A review. *Reviews of Modern*

Plasma Physics, *7*(1), 6, Jan. 2023. ISSN 2367-3192. doi: 10.1007/s41614-022-00111-2.

Maggio, A., Pillitteri, I., Scandariato, G., Lanza, A. F., Sciortino, S., Borsa, F., et al. (2015). Coordinated X-ray and optical observations of Star–Planet interaction in HD 17156. *The Astrophysical Journal Letters*, *811*(1), L2. ISSN 2041-8205. doi: 10.1088/2041-8205/811/1/L2.

Matsuda, K., Terada, N., Katoh, Y., & Misawa, H. (2012). A simulation study of the current-voltage relationship of the Io tail aurora. *Journal of Geophysical Research (Space Physics)*, *117*(A16), 10214. doi: 10.1029/2012JA017790.

Mauk, B. H., & Saur, J. (2007). Equatorial electron beams and auroral structuring at Jupiter. *Journal of Geophysical Research*, *112*(A11), 10221–+. doi: 10.1029/2007JA012370.

Mauk, B. H., Williams, D. J., & Eviatar, A. (2001). Understanding Io's space environment interaction: Recent energetic electron measurements from Galileo. *Journal of Geophysical Research: Space Physics*, *106*(A11), 26195–26208. ISSN 2156-2202. doi: 10.1029/2000JA002508.

Moirano, A., Mura, A., Adriani, A., Dols, V., Bonfond, B., Waite, J. H., et al. (2021). Morphology of the Auroral Tail of Io, Europa, and Ganymede From JIRAM L-Band Imager. *Journal of Geophysical Research: Space Physics*, *126*(9), e2021JA029450. ISSN 2169-9402. doi: 10.1029/2021JA029450.

Moirano, A., Mura, A., Hue, V., et al. (2024). The Infrared Footprint Tracks of Io, Europa and Ganymede at Jupiter Observed by Juno-JIRAM. ESS Open Archive. doi: 10.22541/essoar.168394732.26574509/v1.

Mura, A., Adriani, A., Connerney, J. E. P., Bolton, S., Altieri, F., Bagenal, F., et al. (2018). Juno observations of spot structures and a split tail in Io-induced aurorae on Jupiter. *Science*, *361*(6404), 774–777. ISSN 0036-8075, 1095-9203. doi: 10.1126/science.aat1450.

Ness, N. F., Acunã, M. H., Lepping, R. P., Burlaga, L. F., Behannon, K. W., & Neubauer, F. M. (1979). Magnetic Field Studies at Jupiter by Voyager 1: Preliminary Results. *Science*, *204*(4396), 982–987. doi: 10.1126/science.204.4396.982.

Neubauer, F. (1980). Nonlinear standing Alfvén wave current system at Io: Theory. *Journal of Geophysical Research: Space Physics*, *85*(A3), 1171–1178. ISSN 2156-2202. doi: 10.1029/JA085iA03p01171.

Neubauer, F. M. (1998). The sub-Alfvénic interaction of the Galilean satellites with the Jovian magnetosphere. *Journal of Geophysical Research: Planets*, *103*(E9), 19843–19866. ISSN 2156-2202. doi: 10.1029/97JE03370.

Neubauer, F. M., Backes, H., Dougherty, M. K., Wennmacher, A., Russell, C. T., Coates, A., et al. (2006). Titan's near magnetotail from magnetic field and electron plasma observations and modeling: Cassini flybys TA, TB, and T3. *Journal of Geophysical Research: Space Physics*, *111*(A10). ISSN 2156-2202. doi: 10.1029/2006JA011676.

Pagano, I., Lanza, A. F., Leto, G., Messina, S., Barge, P., & Baglin, A. (2009). CoRoT-2a Magnetic Activity: Hints for Possible Star-Planet Interaction. *Earth, Moon, and Planets*, *105*(2), 373–378. ISSN 1573-0794. doi: 10.1007/s11038-009-9301-3.

Piddington, J. H., & Drake, J. F. (1968). Electrodynamic effects of Jupiter's Satellite Io. *Nature*, *217*:935–937. doi: 10.1038/217935a0.

Pontius, D. H. (2002). The Io current wing. *Journal of Geophysical Research: Space Physics*, *107*(A8), SMP 6–1–SMP 6–12. ISSN 2156-2202. doi: 10.1029/2001JA000331.

Porco, C. C., Helfenstein, P., Thomas, P. C., Ingersoll, A. P., Wisdom, J., West, R., et al. (2006). Cassini Observes the Active South Pole of Enceladus. *Science*, *311*(5766), 1393–1401. doi: 10.1126/science.1123013.

Prangé, R., Rego, D., Southwood, D., Zarka, P., Miller, S., & Ip, W. (1996). Rapid energy dissipation and variability of the lo-Jupiter electrodynamic circuit. *Nature*, *379*(6563), 323–325. ISSN 1476-4687. doi: 10.1038/379323a0.

Pryor, W. R., Rymer, A. M., Mitchell, D. G., Hill, T. W., Young, D. T., Saur, J., et al. (2011). The auroral footprint of Enceladus on Saturn. *Nature*, *472*(7343), 331–333. ISSN 1476-4687. doi: 10.1038/nature09928.

Queinnec, J., & Zarka, P. (1998). Io-controlled decameter arcs and Io-Jupiter interaction. *Journal of Geophysical Research: Space Physics*, *103*(A11), 26649–26666. ISSN 2156-2202. doi: 10.1029/98JA02435.

Ridley, A. J. (2007). Alfvén wings at Earth's magnetosphere under strong interplanetary magnetic fields. *Annales Geophysicae*, *25*(2), 533–542. ISSN 0992-7689. doi: 10.5194/angeo-25-533-2007.

Roth, L., Saur, J., Retherford, K. D., Strobel, D. F., Feldman, P. D., McGrath, M. A., & Nimmo, F. (2014). Transient water vapor at Europa's South Pole. *Science*, *343*(6167), 171–174. ISSN 0036-8075, 1095-9203. doi: 10.1126/science.1247051.

Roth, L., Alday, J., Becker, T. M., Ivchenko, N., & Retherford, K. D. (2017). Detection of a hydrogen corona at Callisto. *Journal of Geophysical Research: Planets*, *122*(5), 1046–1055. ISSN 2169-9100. doi: 10.1002/2017JE005294.

Rymer, A. M., Smith, H. T., Wellbrock, A., Coates, A. J., & Young, D. T. (2009). Discrete classification and electron energy spectra of Titan's varied magnetospheric environment. *Geophysical Research Letters*, *36*(15), L15109. ISSN 1944-8007. doi: 10.1029/2009GL039427.

Sarantos, M., & Slavin, J. A. (2009). On the possible formation of Alfvén wings at Mercury during encounters with coronal mass ejections. *Geophysical Research Letters*, *36*(4). ISSN 1944-8007. doi: 10.1029/2008GL036747.

Saur, J. (2004). A model of Io's local electric field for a combined Alfvénic and unipolar inductor far-field coupling. *Journal of Geophysical Research*, *109*(A18), 1210–+. doi: 10.1029/2002JA009354.

Saur, J. (2018). Electromagnetic Coupling in Star-Planet Systems. In H. J. Deeg and J. A. Belmonte (Eds.), *Handbook of exoplanets* (pp. 1877–1893). Springer International Publishing, Cham, 2018. ISBN 978-3-319-55333-7. doi: 10.1007/978-3-319-55333-7_27.

Saur, J. (2021). Overview of Moon-Magnetosphere interactions. In *Magnetospheres in the solar system* (pp. 575–593). American Geophysical Union (AGU). ISBN 978-1-119-81562-4. doi: 10.1002/9781119815624.ch36. Section: 36.

Saur, J., Neubauer, F. M., Strobel, D. F., & Summers, M. E. (1999). Three-dimensional plasma simulation of Io's interaction with the Io plasma torus: Asymmetric plasma flow.

Journal of Geophysical Research: Space Physics, *104*(A11), 25105–25126. ISSN 2156-2202. doi: 10.1029/1999JA900304.

Saur, J., Grambusch, T., Duling, S., Neubauer, F. M., & Simon, S. (2013). Magnetic energy fluxes in sub-Alfvénic planet star and moon planet interactions. *Astronomy & Astrophysics*, *552*, A119. ISSN 0004-6361, 1432-0746. doi: 10.1051/0004-6361/201118179.

Schilling, N., Neubauer, F. M., & Saur, J. (2008). Influence of the internally induced magnetic field on the plasma interaction of Europa. *Journal of Geophysical Research: Space Physics*, *113*(A3). ISSN 2156-2202. doi: 10.1029/2007JA012842.

Shkolnik, E., Walker, G. A. H., & Bohlender, D. A. (2003, November). Evidence for Planet-induced chromospheric activity on HD 179949. *The Astrophysical Journal*, *597*(2), 1092–1096. ISSN 0004-637X. doi: 10.1086/378583.

Shkolnik, E., Bohlender, D. A., Walker, G. A. H., & Cameron, A. C. (2008). The On/Off Nature of Star-Planet Interactions*. *The Astrophysical Journal*, *676*(1), 628. ISSN 0004-637X. doi: 10.1086/527351.

Shkolnik, E. L., & Llama, J. (2018). Signatures of Star-Planet interactions. In H. J. Deeg and J. A. Belmonte (Eds.), *Handbook of Exoplanets* (pp. 1737–1753). Springer International Publishing, Cham, 2018. ISBN 978-3-319-55333-7. doi: 10.1007/978-3-319-55333-7_20.

Sillanpää, I., & Johnson, R. E. (2015). The role of ion-neutral collisions in Titan's magnetospheric interaction. *Planetary and Space Science*, *108*, 73–86. ISSN 0032-0633. doi: 10.1016/j.pss.2015.01.007.

Sillanpää, I., Kallio, E., Jarvinen, R., & Janhunen, P. (2007). Oxygen ions at Titan's exobase in a Voyager 1-type interaction from a hybrid simulation. *Journal of Geophysical Research: Space Physics*, *112*(A12), A12205. ISSN 2156-2202. doi: 10.1029/2007JA012348.

Simon, S., Wennmacher, A., Neubauer, F. M., Bertucci, C. L., Kriegel, H., Saur, J., et al. (2010). Titan's highly dynamic magnetic environment: A systematic survey of Cassini magnetometer observations from flybys TA-T62. *Planetary and Space Science*, *58*(10), 1230–1251. ISSN 0032-0633. doi: 10.1016/j.pss.2010.04.021.

Simon, S., Saur, J., Kriegel, H., Neubauer, F. M., Motschmann, U., & Dougherty, M. K. (2011). Influence of negatively charged plume grains and hemisphere coupling currents on the structure of Enceladus' Alfvén wings: Analytical modeling of Cassini magnetometer observations. *Journal of Geophysical Research: Space Physics*, *116*(A4). ISSN 2156-2202. doi: 10.1029/2010JA016338.

Simon, S., Kriegel, H., Saur, J., Wennmacher, A., Neubauer, F. M., Roussos, E., et al. (2012). Analysis of Cassini magnetic field observations over the poles of Rhea. *Journal of Geophysical Research: Space Physics*, *117*(A7), A07211. ISSN 2156-2202. doi: 10.1029/2012JA017747.

Simon, S., Addison, P., & Liuzzo, L. (2022). Formation of a displaced plasma wake at Neptune's Moon Triton. *Journal of Geophysical Research: Space Physics*, *127*(1), e2021JA029958. ISSN 2169-9402. doi: 10.1029/2021JA029958.

D. Snowden, R. V. Yelle, M. Galand, A. J. Coates, A. Wellbrock, G. H. Jones, & Lavvas, P. (2013, September). Auroral electron precipitation and flux tube erosion in Titan's upper atmosphere. *Icarus*, *226*(1), 186–204. ISSN 0019-1035. doi: 10.1016/j.icarus.2013.05.021.

Strugarek, A. (2018). Models of Star-Planet magnetic interaction. In H. J. Deeg and J. A. Belmonte (Eds.), *Handbook of Exoplanets* (pp. 1833–1855). Springer International Publishing, Cham, 2018. ISBN 978-3-319-55333-7. doi: 10.1007/978-3-319-55333-7_25.

Sulaiman, A. H., Kurth, W. S., Hospodarsky, G. B., Averkamp, T. F., Ye, S.-Y., Menietti, J. D., et al. (2018). Enceladus auroral hiss emissions during Cassini's Grand Finale. *Geophysical Research Letters*, *45*(15), 7347–7353. ISSN 1944-8007. doi: 10.1029/2018GL078130.

Sulaiman, A. H., Hospodarsky, G. B., Elliott, S. S., Kurth, W. S., Gurnett, D. A., Imai, M., et al. (2020). Wave-particle interactions associated with Io's auroral footprint: Evidence of Alfvén, ion cyclotron, and whistler modes. *Geophysical Research Letters*, *47*(22), e2020GL088432. ISSN 1944-8007. doi: 10.1029/2020GL088432.

Sulaiman, A. H., Szalay, J. R., Clark, G., Allegrini, F., Bagenal, F., Brennan, M. J., et al. (2023). Poynting fluxes, field-aligned current densities, and the efficiency of the Io-Jupiter electrodynamic interaction. *Geophysical Research Letters*, *50*(10), e2023GL103456. ISSN 1944-8007. doi: 10.1029/2023GL103456.

Szalay, J. R., Bonfond, B., Allegrini, F., Bagenal, F., Bolton, S., Clark, G., et al. (2018). In situ observations connected to the Io footprint tail aurora. *Journal of Geophysical Research: Planets*, *123*(11), 3061–3077. ISSN 2169-9100. doi: 10.1029/2018JE005752.

Szalay, J. R., Allegrini, F., Bagenal, F., Bolton, S. J., Bonfond, B., Clark, G., et al. (2020a). Alfvénic acceleration sustains Ganymede's footprint tail aurora. *Geophysical Research Letters*, *47*(3), e2019GL086527. ISSN 1944-8007. doi: https://doi.org/10.1029/2019GL086527.

Szalay, J. R., Allegrini, F., Bagenal, F., Bolton, S. J., Bonfond, B., Clark, G., et al. (2020b). A new framework to explain changes in Io's footprint tail electron fluxes. *Geophysical Research Letters*, *47*(18), e2020GL089267. ISSN 1944-8007. doi: 10.1029/2020GL089267.

Szalay, J. R., Bagenal, F., Allegrini, F., Bonfond, B., Clark, G., Connerney, J. E. P., et al. (2020c). Proton acceleration by Io's Alfvénic interaction. *Journal of Geophysical Research: Space Physics*, *125*(1), e2019JA027314. ISSN 2169-9402. doi: 10.1029/2019JA027314.

Vasavada, A. R., Bouchez, A. H., Ingersoll, A. P., Little, B., Anger, C. D., & The Galileo SSI Team. (1999). Jupiter's visible aurora and Io footprint. *Journal of Geophysical Research*, *104*, 27133–+.

Vasyliūnas, V. M. (2016). Physical origin of pickup currents. *Annales Geophysicae*, *34* (1), 153–156. ISSN 0992-7689. doi: 10.5194/angeo-34-153-2016.

Viswanath, G., Narang, M., Manoj, P., Mathew, B., & Kartha, S. S. (2020, May). A statistical search for Star-Planet interaction in the ultraviolet using GALEX. *The Astronomical Journal*, *159*, 194. ISSN 0004-6256. doi: 10.3847/1538-3881/ab7d3b.

Walker, G. A. H., Croll, B., Matthews, J. M., Kuschnig, R., Huber, D., Weiss, W. W., et al. (2008). MOST detects variability on τ Bootis A possibly induced by its planetary

companion. *Astronomy and Astrophysics*, *482*, 691–697. doi: 10.1051/0004-6361:20078952.

Wannawichian, S., Clarke, J. T., & Pontius, D. H. (2008). Interaction evidence between Enceladus' atmosphere and Saturn's magnetosphere. *Journal of Geophysical Research: Space Physics*, *113*(A7). ISSN 2156-2202. doi: 10.1029/2007JA012899.

Webster, D. L., Alksne, A. Y., & Whitten, R. C. (1972, June). Does Io's ionosphere influence Jupiter's Radio bursts? *The Astrophysical Journal*, *174*, 685. ISSN 0004-637X. doi: 10.1086/151530.

Wei, H. Y., Russell, C. T., Wahlund, J.-E., Dougherty, M. K., Bertucci, C., Modolo, R., et al. (2007). Cold ionospheric plasma in Titan's magnetotail. *Geophysical Research Letters*, *34*(24). ISSN 1944-8007. doi: 10.1029/2007GL030701.

Williams, D. J., & Mauk, B. (1997). Pitch angle diffusion at Jupiter's moon Ganymede. *Journal of Geophysical Research: Space Physics*, *102*(A11), 24283–24287. ISSN 2156-2202. doi: 10.1029/97JA02260.

Williams, D. J., & Thorne, R. M. (2003). Energetic particles over Io's polar caps. *Journal of Geophysical Research: Space Physics*, *108* (A11), 1397. ISSN 2156-2202. doi: 10.1029/2003JA009980.

Williams, D. J., Mauk, B. H., McEntire, R. E., Roelof, E. C., Armstrong, T. P., Wilken, B., et al. (1996). Electron beams and ion composition measured at lo and in its Torus. *Science*, *274*, 401–403.

Williams, D. J., Mauk, B., & McEntire, R. W. (1997). Trapped electrons in Ganymede's magnetic field. *Geophysical Research Letters*, *24*(23), 2953–2956. ISSN 1944-8007. doi: 10.1029/97GL03003.

Williams, D. J., Mauk, B. H., McEntire, R. W., Roelof, E. C., Armstrong, T. P., Wilken, B., et al. (1997). Energetic particle signatures at Ganymede: Implications for Ganymede's magnetic field. *Geophysical Research Letters*, *24* (17), 2163–2166. ISSN 1944-8007. doi: 10.1029/97GL01931.

Wright, A. N. (1987). The interaction of Io's Alfven waves with the Jovian magnetosphere. *Journal of Geophysical Research: Space Physics*, *92*(A9), 9963–9970. ISSN 2156-2202. doi: 10.1029/JA092iA09p09963.

Wright, A. N., & Southwood, D. J. (1987). Stationary Alfvenic structures. *Journal of Geophysical Research*, *92*, 1167–1175.

Zarka, P. (1998). Auroral radio emissions at the outer planets: Observations and theories. *Journal of Geophysical Research: Planets*, *103* (E9), 20159–20194. ISSN 0148-0227. doi: 10.1029/98JE01323.

Zhang, H., Khurana, K. K., Kivelson, M. G., Fatemi, S., Holmström, M., Angelopoulos, V., et al. (2016). Alfvén wings in the lunar wake: The role of pressure gradients. *Journal of Geophysical Research: Space Physics*, *121*(11), 10,698–10,711. ISSN 2169-9402. doi: 10.1002/2016JA022360.

Zhou, H., Tóth, G., Jia, X., & Chen, Y. (2020). Reconnection-driven dynamics at Ganymede's upstream magnetosphere: 3-D Global Hall MHD and MHD-EPIC simulations. *Journal of Geophysical Research: Space Physics*, *125*(8), e2020JA028162. ISSN 2169-9402. doi: https://doi.org/10.1029/2020JA028162.

Zimmer, C., Khurana, K. K., & Kivelson, M. G. (2000). Subsurface oceans on Europa and Callisto: Constraints from Galileo magnetometer observations. *Icarus*, *147*(2), 329–347. ISSN 0019-1035. doi: 10.1006/icar.2000.6456.